

Design and hedging of unit linked life insurance with environmental factors

Katia Colaneri ^{*1}, Alessandra Cretarola ^{†2}, Edoardo Lombardo^{‡1}, and Daniele Mancinelli^{§1}

¹*Department of Economics and Finance, University of Rome Tor Vergata.*

²*Department of Economics, University of Pescara.*

September 9, 2025

Abstract

We study the problem of designing and hedging unit-linked life policies whose benefits depend on an investment fund that incorporates environmental criteria in its selection process. Offering these products poses two key challenges: constructing a green investment fund and developing a hedging strategy for policies written on that fund. We address these two problems separately. First, we design a portfolio selection rule driven by firms' carbon intensity that endogenously selects assets and avoids ad hoc pre-screens based on ESG scores. The effectiveness of our new portfolio selection method is tested using real market data. Second, we adopt the perspective of an insurance company issuing unit-linked policies written on this fund. Such contracts are exposed to market, carbon, and mortality risk, which the insurer seeks to hedge. Due to market incompleteness, we address the hedging problem via a quadratic approach aimed at minimizing the tracking error. We also make a numerical analysis to assess the performance of the hedging strategy. For our simulation study, we use an efficient weak second-order scheme that allows for variance reduction.

Keywords: Sustainable investments; Unit linked; Carbon intensity; Risk-minimization.

JEL classification: C61, G11, G22.

AMS classification: 49L12, 60J76, 91B16, 91G20.

1 Introduction

Recent studies, including Hartzmark and Sussman (2019), Lagerkvist et al. (2020), and Anquetin et al. (2022), show that climate change is increasingly recognized as a systemic risk by global stakeholders. As a result, institutional investors have begun to incorporate ESG criteria into portfolio construction and to evaluate the environmental and social footprint of their investments. For example, Peng et al. (2024) reports that the Chinese Government Pension Investment Fund has allocated 163 trillion yen to passive ESG index products, while the California Public Employees' Retirement System follows a "social change investment" approach aligned with ESG principles. Such a change has also involved the insurance sector, which is increasingly integrating ESG principles into both strategic decision-making and the design of insurance-based investment products (IBIPs). Among these, unit linked

*katia.colaneri@uniroma2.it

†alessandra.cretatola@unich.it

‡edoardo.lombardo@uniroma2.it

§Corresponding author: daniele.mancinelli@uniroma2.it

insurance policies incorporating ESG characteristics have seen a sharp increase, as documented by recent surveys. In particular, EIOPA (2023) reported a 24% increase in the number of IBIPs classified under Articles 8 and 9 of the Sustainable Finance Disclosure Regulation (SFDR).⁽¹⁾ Moreover, a study carried out by IVASS (2024), based on a sample of 106 IBIPs offered by 18 insurers, found that 92% of unit linked life insurance policies are classified under Article 8 of the SFDR.

Although ESG factors encompass several aspects, this paper focuses on greenhouse gas (GHG) emissions. Indeed, a central concern in the low-carbon transition is managing carbon risk, which includes regulatory, market, and reputational components. Institutional investors, including insurers, aim to reduce their carbon footprint for two main reasons: to balance short-term gains from carbon-intensive assets with long-term risks associated with climate change, and to address increasing public scrutiny over the environmental impact of their investments. Therefore, accounting for carbon risk into portfolio and product decisions is thus critical for long-term financial sustainability. This requires consistent emission metrics; in this study we adopt the carbon intensity approach by Hellmich and Kiesel (2021) over the alternative Brown-Green Score proposed by Gorgen et al. (2020).

These developments raise important questions regarding the operational and financial implications for insurance companies offering unit linked life insurance policies whose underlying investment funds explicitly account for carbon risk. Such products present challenges on two distinct levels: the construction of the “green” investment fund, and the development of a hedging strategy for the unit linked policy whose benefit is related to that fund. The aim of this work is to address these two problems. In the first part, we adopt the point of view of a fund manager and propose a novel portfolio selection methodology capable of properly accounting for carbon risk in an endogenous way. In the second part, we change the role to that of an insurance company issuing unit linked life insurance policies written on that fund. The insurer is simultaneously exposed to market risk, carbon risk, and mortality risk. Since neither carbon risk nor mortality risk is fully hedgeable, the insurance company cannot replicate the policy’s payoff through a self-financing strategy. This results in a residual loss, which we aim to minimize. Specifically, we adopt a quadratic criterion that minimizes the tracking error.

The first step of our study aims to develop a new portfolio selection method that integrates sustainability criteria, contributing to a growing strand of literature. A seminal contribution is provided by Andersson et al. (2016), who proposes excluding high-carbon stocks to minimize tracking error and cut the portfolio’s carbon footprint by half, while potentially outperforming benchmarks. Bolton et al. (2022) extend this approach by including an additional constraint that aligns portfolios with the Paris Agreement, maintaining low tracking error and reducing emissions over time. Alternative approaches retain the full investment universe and impose sustainability constraints during optimization. Among these we mention Le Guenedal and Roncalli (2023), who select portfolios to minimize benchmark deviation, while capping overall carbon risk. De Spiegeleer et al. (2023) apply constraints on both carbon intensity and ESG ratings, finding that low-ESG portfolios may outperform short-term, while high-ESG portfolios excel over longer time horizons. They also observe that strict carbon limits have a minimal impact on performance.

Unlike prior studies, we do not pre-select assets nor impose carbon constraints. Instead, we penal-

⁽¹⁾SFDR classifies financial products based on the sustainability features. Article 8 products promote environmental or social characteristics, although sustainability is not their primary objective. Article 9 products, instead, have sustainable investment as their explicit goal, contributing to environmental goals defined by the EU Taxonomy.

ize the terminal portfolio value based on each asset’s carbon intensity and realized volatility, scaled by a time-varying factor reflecting the manager’s carbon aversion. We model asset prices via geometric Brownian motion, and propose several plausible dynamics to model carbon intensities. Using dynamic programming, we derive closed-form optimal portfolio weights that maximize the expected CRRA utility of the carbon-penalized terminal value. This yields a value function that is characterised as the solution of a Hamilton–Jacobi–Bellman (HJB) partial differential equation (PDE). Our method embeds sustainability directly into preferences, balancing market risk with carbon aversion through an exogenous parameter. Moreover, our method has the advantage of allowing for a trade-off between market risk and the carbon intensity of each asset in the portfolio. Indeed, if the expected return (resp., the volatility) of a carbon-intensive asset is sufficiently high (resp., low), it may compensate for the adverse effects of carbon risk. We empirically validate the model using data from 34 S&P 500 stocks, calibrate parameters, and analyze the impact of varying carbon aversion. Results show that greater aversion reduces investment in carbon-intensive stocks and lowers portfolio carbon intensity, confirming the model’s ability to flexibly integrate environmental goals into investment decisions without rigid sustainability constraints.

In the second part of the article, we change perspective and adopt the viewpoint of an insurance company issuing green unit linked life insurance contracts, that is, policies whose benefits depend both on the performance of a carbon-sensitive investment fund and on the policyholder’s lifetime. In this context, the insurer is simultaneously exposed to market risk, mortality risk, and carbon risk. Since neither carbon intensity nor mortality can be hedged using traded financial instruments, the market is incomplete, and the contract’s payoff cannot be perfectly replicated. To address this, we adopt a quadratic hedging criterion aimed at identifying a replication strategy that minimizes the cost of hedging. Specifically, we resort to the (local) risk minimization approach (see, for example, Schweizer (2001); Møller (2001); Vandaele and Vanmaele (2008)), which is particularly well-suited to applications in the insurance context. We derive theoretical results for the computation of the risk minimizing hedging strategy for unit-linked pure endowment, term insurance, and endowment insurance contracts. The paper concludes with a simulation study in which we compare the performance of different hedging strategies, namely, dynamic hedging via risk minimization, static hedging, and no hedging. The numerical results demonstrate that dynamic hedging strategies substantially reduce losses, both relative to static hedging, where a strategy is fixed at time $t = 0$ and never adjusted, and to the case in which the insurance company does not hedge at all. Our findings indicate that dynamic risk-mitigation techniques can be used as powerful tools for managing potential losses associated with life insurance policies. To conduct the simulation study, we apply a methodology that leads to variance reduction, thereby enabling efficient pricing and hedging of the contracts. This methodology consists of two main components: (i) employing efficient simulation schemes for the fund and its underlying carbon intensity process, and (ii) applying a conditioning technique.

The remainder of this article is organized as follows. Section 2 introduces the market model, the modeling assumptions. Section 3 introduces and solves the the fund’s manager optimization problem and includes an empirical illustration based on real market data. In Section 6, we shift to the insurer’s point of view and address the problem of hedging green unit linked life insurance contracts in an incomplete market. Section 7 presents a simulation scheme for the carbon-penalized investment fund and numerical illustrations of risk-minimizing strategies for different types of insurance contracts. Section 8 poses the conclusions.

2 Model setup

Let $(\Omega^M, \mathbb{F}, \mathbb{P}^M)$ be a fixed probability and a finite time horizon T coinciding with the terminal time of an investment. We also introduce a \mathbb{P}^M -complete and right-continuous filtration $\mathbb{F} = \{\mathcal{F}_t\}_{t \in [0, T]}$, and we assume that all processes below are \mathbb{F} -adapted. We consider a financial market model consisting of d stocks with price processes $\mathbf{S} = \{\mathbf{S}_t\}_{t \in [0, T]}$ in \mathbb{R}_+^d , and one risk-free asset B , that are traded continuously on $[0, T]$. The dynamics of the risk-free are given by

$$dS_t^0 = rS_t^0 dt, \quad S_0^0 = 1,$$

where $r > 0$ denotes the constant risk-free interest rate. The price dynamics of the risky assets \mathbf{S} are given by

$$d\mathbf{S}_t = \text{diag}(\mathbf{S}_t) (\boldsymbol{\mu} dt + \boldsymbol{\Sigma} d\mathbf{Z}_t), \quad \mathbf{S}_0 \in \mathbb{R}^+, \quad (2.1)$$

where $\boldsymbol{\mu} \in \mathbb{R}^d$ is the vector of constant drift rates, $\mathbf{Z} = \{\mathbf{Z}_t\}_{t \in [0, T]}$ is a standard d -dimensional \mathbb{F} -Brownian motion with independent component, and $\boldsymbol{\Sigma}\boldsymbol{\Sigma}^\top$ is the variance-covariance matrix of asset prices.⁽²⁾ Stocks are assumed to be issued by firms with different levels of carbon emissions, measured by carbon intensity. A firm's carbon intensity is defined as the ratio between the total greenhouse gas emissions in metric tonnes of CO₂ and total revenues (in USD millions). Let $\mathbf{C} = (C_1, \dots, C_d)^\top$, where $C_i = \{C_{i,t}\}_{t \in [0, T]}$ denotes the carbon intensity process of the i -th firm. We assume that \mathbf{C} is a d -dimensional Markov process with mutually independent components, and we denote by $\mathcal{L}^{\mathbf{C}}$ its infinitesimal generator. Moreover, we assume that C_i is independent of \mathbf{Z} , for every $i = 1, \dots, d$.

Remark 2.1. *The assumption that the \mathbf{C} has mutually independent components reflects the idea that firm-level carbon intensity evolves largely as an idiosyncratic process, shaped by heterogeneous technologies, sector-specific constraints, and individual decarbonization strategies. Moreover, the independence between C_i and \mathbf{Z} for every $i = 1, \dots, d$ is supported by empirical findings from Bolton and Kacperczyk (2021), who show that stock performance is significantly related to the absolute level of firm emissions, but not to carbon intensity. In particular, carbon intensity does not appear to be priced by the market, indicating that it is largely uncorrelated with the drivers of financial returns. To further investigate the relationship between carbon intensity and financial performance, we run a cross-sectional regression of annualized mean log-returns on carbon intensity using the dataset employed in our empirical analysis (see Section 5). Table 2.1 reports the results of the regression:*

$$\text{mean log-return}_i = \beta_0 + \beta_1 \cdot \text{carbon intensity}_i, \quad (2.2)$$

for every $i = 1, \dots, d$. The corresponding scatter plot, along with the estimated regression line, is shown in Figure 2.1. As shown in table 2.1, the slope coefficient is negative and statistically different from zero, but economically negligible. This result suggests a weak negative relation between carbon intensity and expected average returns, but the effect is too small to be of practical relevance. Hence, in line with the findings of Bolton and Kacperczyk (2021), our data also suggest that carbon intensity has limited explanatory power for expected returns.

	Estimate	S.E.	t-stat	p-value
$\hat{\beta}_0$	0.068831	0.0030407	22.637	2.0416E-74
$\hat{\beta}_1$	-1.77E-05	5.2761E-06	-3.3628	0.00084348

Table 2.1: OLS estimation results for the regression defined by equation (2.2).

⁽²⁾ $\boldsymbol{\Sigma} = \mathbf{L}\mathbf{D}$ where $\mathbf{D} = \text{diag}(\sigma_1, \dots, \sigma_d)$ with $\sigma_i > 0$ for all $i = 1, \dots, d$, and \mathbf{L} is the lower triangular matrix obtained through Cholesky decomposition of the correlation matrix of asset prices $\boldsymbol{\rho} = (\rho_{i,j})_{i,j=1,\dots,d}$, so that $\boldsymbol{\rho} = \mathbf{L}\mathbf{L}^\top$.

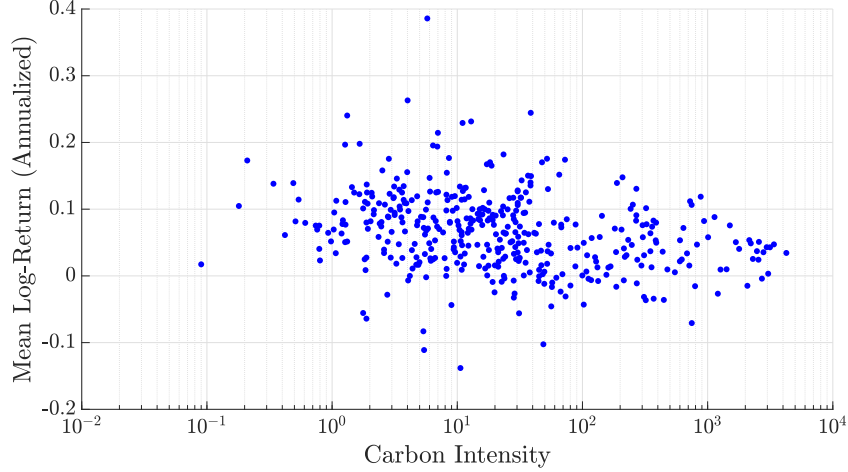


Figure 2.1: Scatter plot of annualized mean log-returns versus carbon intensity (on log scale) for the S&P500 stocks. Note that the x -axis uses a logarithmic scale, which may slightly distort the visual effect of the sparsity of the points.

3 Optimal carbon-penalized investment strategy

We adopt the perspective of a fund manager operating in the financial market described in Section 2, whose goal is to construct an investment fund that accounts for carbon risk. Let $X^\pi = \{X_t^\pi\}_{t \in [0, T]}$ be the value of a self-financing portfolio and let $\pi = (\pi_1, \dots, \pi_d)^\top$ where $\pi_i = \{\pi_{i,t}\}_{t \in [0, T]}$ denote fraction of the wealth invested in the risky assets \mathbf{S} . Consequently, the percentage of wealth invested in the riskless asset is $1 - \pi_i^\top \mathbf{1}$, for every $t \in [0, T]$. We introduce now the suitable set of strategies.

Definition 3.1. A \mathbb{F} -admissible portfolio strategy is a self-financing, \mathbb{F} -predictable strategy π such that $\pi \in [-\Xi, \Xi]^d$ for some $\Xi > 0$. The set of \mathbb{F} -admissible strategies is denoted by \mathcal{A} .

Remark 3.2. For technical reasons, we have restricted the set of strategies to a compact set. This is not a limitation, since the optimal strategy turns out to be bounded, as we show later in this section. Therefore, for a sufficiently large compact set, the optimal strategy lies in the interior of the admissible set.

For every $\pi \in \mathcal{A}$, the dynamics of the portfolio X^π is given by

$$\frac{dX_t^\pi}{X_t^\pi} = \left[r + \pi_t^\top (\boldsymbol{\mu} - \mathbf{1}r) \right] dt + \pi_t^\top \boldsymbol{\Sigma} d\mathbf{Z}_t, \quad X_0^\pi = x_0.$$

The objective is to maximize the expected utility from terminal wealth in a carbon-penalized setting, preventing the fund manager from pursuing risky assets characterized by a high carbon intensity. Such penalization is applied to the terminal portfolio value, and it is assumed to be proportional to the riskiness of stocks, measured according to their realized volatility. The idea of penalization is inspired by Rogers (2013), under a slightly different definition (see Remark 3.4). The carbon-penalized portfolio value at maturity is given by

$$\tilde{X}_T^\pi = X_T^\pi \exp \left(-\frac{1}{2} \int_0^T \pi_s^\top \left(\mathbf{e}(s, \mathbf{C}_s) \odot \mathbf{D}\mathbf{D}^\top \right) \pi_s ds \right),$$

where \odot denotes the elementwise (Hadamard) product, and $\mathbf{e}(t, \mathbf{C}_t) = [\varepsilon_1(t, C_{1,t}), \dots, \varepsilon_d(t, C_{d,t})]^\top$ is the vector containing the fund manager's carbon aversion for each stock in the portfolio, such that

$$\mathbb{E}^{\mathbb{P}^M} \left[\int_0^T \varepsilon_i(s, C_{i,s}) ds \right] < \infty,$$

for every $i = 1, \dots, d$. In particular, the carbon aversion of the i -th stock is given by

$$\varepsilon_i(t, C_{i,t}) = \alpha_i(t)C_{i,t}\mathbb{1}_{\{C_{i,t}>0\}}, \quad t \in [0, T], \quad (3.1)$$

where $\alpha_i(\cdot) : [0, T] \rightarrow [0, +\infty)$ for every $i = 1, \dots, d$. Specifically, α_i captures the time-varying environmental preferences of the fund manager with respect to the i -th firm, reflecting how strongly the carbon emissions of that firm are penalized in the investment decision. A higher α_i corresponds to a greater carbon aversion with respect to the i -th asset and thus a stronger shift toward low-emission investments. It is worth noting that our penalization scheme is not necessarily stock-specific. For instance, the fund manager may choose to assign the same penalization to all stocks, or adopt a sector-based approach where the same α is applied to all stocks within a given sector. Moreover, α_i is time-varying, allowing the penalization scheme to evolve consistently with long-term environmental targets. In particular, it can be aligned with exogenous sustainability goals (e.g., regulatory guidelines or Net Zero emission commitments), enabling the investment strategy to dynamically adjust its sensitivity to carbon risk as these objectives become more (or less) binding over time.

Remark 3.3. *Recent contributions in the literature acknowledge the possibility that firms may report net-negative carbon emissions for instance due to the deployment of carbon removal technologies, such as Direct Air Capture (DAC) or Bioenergy with Carbon Capture and Storage (BECCS); the implementation of nature-based solutions, including afforestation, reforestation; the purchase of high-quality certified offsets that correspond to verifiable and additional carbon removals (see, e.g., Bhatia et al. (2025) and Verbist et al. (2025)). Motivated by this evidence, our model allows the carbon intensity process $C_{i,t}$ to take negative values, and no penalization is applied when this occurs (see equation (3.1)). From a modeling perspective, one may also extend our study to include incentives for stocks with negative carbon intensity. However, such an approach may be subject to criticism, as it could result in greenwashing practices.*

Remark 3.4. *The proposed penalization incorporates sustainability into the fund manager preferences by enhancing her risk aversion specifically toward stocks with high carbon intensity. Unlike Rogers (2013), this adjustment does not act on the variance-covariance matrix. The reason is that negative correlations among stocks with high carbon intensity would mitigate the penalization, thereby misrepresenting the manager’s true risk preferences. To avoid such distortions, the penalization relies solely on each asset’s realized variance. Furthermore, in contrast to the existing literature (e.g., Bolton et al. (2022); Le Guenedal and Roncalli (2023)), we do not impose a binding sustainability constraint on the investment strategy. Instead, our method enables a trade-off between carbon intensity and market risk: a stock with high carbon intensity may still be held in the portfolio if its low volatility and large return sufficiently offset its carbon risk.*

The carbon penalization admits two complementary interpretations. First, it is analogous to a proportional transaction cost imposed on carbon-intensive securities. In this interpretation, the manager weighs the benefit of, e.g. a higher risk premium, against the reputational or regulatory cost of holding assets with high carbon intensity that may prevent the fund from being classified as “green”. Second, the penalization can be viewed as an endogenous adjustment to the manager’s degree of risk aversion. This, in turn, transforms the optimization problem into one with stochastic risk aversion, where the effective degree of risk aversion is the sum of the utility-based parameter and the carbon penalization term. As a result, exposure to carbon-intensive assets is naturally reduced. The implications of this mechanism for optimal strategies are discussed in details in Example 3.7, Remark 3.8, and Section 5 below.

It follows from Itô's formula that the dynamics of $\tilde{X}^\pi = \{\tilde{X}_t^\pi\}_{t \in [0, T]}$ is given by

$$\frac{d\tilde{X}_t^\pi}{\tilde{X}_t^\pi} = \left[r + \boldsymbol{\pi}_t^\top (\boldsymbol{\mu} - \mathbf{1}r) - \frac{1}{2} \boldsymbol{\pi}_t^\top \left(\mathbf{e}(t, \mathbf{C}_t) \odot \mathbf{D}\mathbf{D}^\top \right) \boldsymbol{\pi}_t \right] dt + \boldsymbol{\pi}_t^\top \boldsymbol{\Sigma} d\mathbf{Z}_t, \quad \tilde{X}_0^\pi = x_0. \quad (3.2)$$

Assuming that the fund manager is endowed with a CRRA utility function U , we address the following optimization problem

$$\text{Maximize } \mathbb{E}_{t,x,\mathbf{c}}^{\mathbb{P}^M} [U(\tilde{X}_T^\pi)], \text{ over all } \boldsymbol{\pi} \in \mathcal{A}, \quad (3.3)$$

where

$$U(x) = \begin{cases} \frac{x^{1-\delta}}{1-\delta}, & \delta \in (0, 1) \cup (1, +\infty), \\ \log(x), & \delta = 1, \end{cases}$$

with δ being the fund manager risk aversion parameter. Here, $\mathbb{E}_{t,x,\mathbf{c}}$ denotes the conditional expectation given $\tilde{X}_t = x$ and $\mathbf{C}_t = \mathbf{c}$. The value function of the optimization problem (3.3), is given by

$$v(t, x, \mathbf{c}) := \sup_{\boldsymbol{\pi} \in \mathcal{A}} \mathbb{E}_{t,x,\mathbf{c}}^{\mathbb{P}^M} [U(\tilde{X}_T^\pi)]. \quad (3.4)$$

The problem is solved by employing the dynamic programming principle. We denote by \mathcal{L} the infinitesimal generator of the process $(\tilde{X}_t^\pi, \mathbf{C}_t)$, that is

$$\begin{aligned} \mathcal{L}F(t, x, \mathbf{c}) = & x \left[r + \boldsymbol{\pi}^\top (\boldsymbol{\mu} - \mathbf{1}r) - \frac{1}{2} \boldsymbol{\pi}^\top \left(\mathbf{e}(t, \mathbf{c}) \odot \mathbf{D}\mathbf{D}^\top \right) \boldsymbol{\pi} \right] \partial_x F(t, x, \mathbf{c}) \\ & + \frac{x^2}{2} \boldsymbol{\pi}^\top \boldsymbol{\Sigma} \boldsymbol{\Sigma}^\top \boldsymbol{\pi} \partial_x^2 F(t, x, \mathbf{c}) + \mathcal{L}^{\mathbf{C}} F(t, x, \mathbf{c}), \end{aligned}$$

for every regular function F and any constant control $\boldsymbol{\pi} \in \mathcal{A}$, where $\mathcal{L}^{\mathbf{C}}$ denotes the infinitesimal generator of \mathbf{C}_t . We consider the following Hamilton-Jacobi-Bellman equation

$$\begin{cases} \sup_{\boldsymbol{\pi} \in \mathcal{A}} \partial_t v(t, x, \mathbf{c}) + \mathcal{L}v(t, x, \mathbf{c}) = 0, & (t, x, \mathbf{c}) \in [0, T) \times \mathbb{R}_+ \times \mathcal{D}, \\ v(T, x, \mathbf{c}) = U(x), & (x, \mathbf{c}) \in \mathbb{R}_+ \times \mathcal{D}. \end{cases} \quad (3.5)$$

In the sequel, we prove that the value function, defined in equation (3.4), solves the equation (3.5). We begin our analysis with a verification result. Within the discussion of the verification theorem we assume quite general dynamics for the carbon intensity process that can accommodate several interesting examples, discussed in Section 4. In particular we assume that \mathbf{C} has a semimartingale decomposition given by

$$\mathbf{C}_t = \mathbf{C}_0 + \int_0^t \boldsymbol{\Gamma}_s ds + \mathbf{M}_t^{cont} + \mathbf{M}_t^{disc},$$

where $\{\mathbf{M}_t^{cont}\}_{t \in [0, T]}$ and $\{\mathbf{M}_t^{disc}\}_{t \in [0, T]}$ are d -dimensional continuous and discontinuous martingales. Moreover we assume that the discontinuous martingale admits the representation

$$d\mathbf{M}_t^{disc} = \int_{\mathcal{Z}} \mathbf{z} (m(dt, d\mathbf{z}) - \nu_t(d\mathbf{z})dt),$$

for some set $\mathcal{Z} \subset \mathbb{R}^d$, where $m([0, t] \times E) = \sum_{s \leq t} \mathbf{1}_{\{\mathbf{C}_s - \mathbf{C}_{s-} \in E\}}$ counts the jumps of \mathbf{C} in $[0, t]$ with sizes in the set $E \subset \mathcal{Z}$ and $\nu_t(d\mathbf{z})$ is the compensator of $m(dt, d\mathbf{z})$, which satisfies $\mathbb{E}^{\mathbb{P}^M} [\int_0^T \nu_s(\mathcal{Z}) ds] < \infty$. To avoid excessive technicalities we assume that \mathcal{Z} is a compact subset of \mathbb{R}^d .

Theorem 3.5 (Verification Theorem). *Suppose that $w(t, x, \mathbf{c})$ is a classical solution of the Hamilton-Jacobi-Bellman equation (3.5) and that $|w(t, x, \mathbf{c})| \leq \bar{k} (1 + |x| + |x|^{1-\delta})$ for some constant $\bar{k} > 0$. Then:*

(i) $w(t, x, \mathbf{c}) \geq v(t, x, \mathbf{c})$ for all $0 \leq t \leq T$, $(x, \mathbf{c}) \in \mathbb{R}_+ \times \mathcal{D}$;

(ii) if $\boldsymbol{\pi}^* = \{\boldsymbol{\pi}_t^*\}_{t \in [0, T]}$ is a maximizer of the HJB-equation, $\boldsymbol{\pi}_s^* = \arg \max\{\partial_t w(t, x, \mathbf{c}) + \mathcal{L}w(t, x, \mathbf{c})\}$ for all $s \in [t, T]$, where $\tilde{X}^{\boldsymbol{\pi}^*}, \mathbf{C}, \boldsymbol{\pi}^*$ solve (3.2), then $w(t, x, \mathbf{c}) = v(t, x, \mathbf{c})$. In particular, $\boldsymbol{\pi}^*$ is an optimal portfolio strategy.

Proof. See Appendix A.1. □

Theorem 3.6. *Let $\varphi(t, \mathbf{c})$ be the unique classical solution to the Cauchy problem*

$$\begin{cases} \partial_t \varphi(t, \mathbf{c}) + \mathcal{L}^{\mathbf{C}} \varphi(t, \mathbf{c}) + H(t, \mathbf{c}) \varphi(t, \mathbf{c}) = f(t, \mathbf{c}), & (t, \mathbf{c}) \in [0, T] \times \mathcal{D}, \\ \varphi(T, \mathbf{c}) = \mathbf{1}_{\{\delta \in (0, 1) \cup (1, +\infty)\}}, & \mathbf{c} \in \mathcal{D}, \end{cases} \quad (3.6)$$

where the functions $H(t, \mathbf{c})$ and $f(t, \mathbf{c})$ are defined as follows:

$$\begin{aligned} H(t, \mathbf{c}) &:= (1 - \delta) \left[r + \frac{1}{2} (\boldsymbol{\mu} - \mathbf{1}r)^\top \left(\delta \boldsymbol{\Sigma} \boldsymbol{\Sigma}^\top + \mathbf{e}(t, \mathbf{c}) \odot \mathbf{D} \mathbf{D}^\top \right)^{-1} (\boldsymbol{\mu} - \mathbf{1}r) \right], \\ f(t, \mathbf{c}) &:= (\boldsymbol{\mu} - \mathbf{1}r)^\top \left(\boldsymbol{\Sigma} \boldsymbol{\Sigma}^\top + \mathbf{e}(t, \mathbf{c}) \odot \mathbf{D} \mathbf{D}^\top \right)^{-1} (\boldsymbol{\mu} - \mathbf{1}r) \mathbf{1}_{\{\delta=1\}}. \end{aligned}$$

Then, there exists $\Xi > 0$ such that the optimal investment strategy is given by

$$\boldsymbol{\pi}^*(t, \mathbf{c}) = \left(\delta \boldsymbol{\Sigma} \boldsymbol{\Sigma}^\top + \mathbf{e}(t, \mathbf{c}) \odot \mathbf{D} \mathbf{D}^\top \right)^{-1} (\boldsymbol{\mu} - \mathbf{1}r) \in [-\Xi, \Xi]^d, \quad (3.7)$$

and the value function satisfies

$$v(t, x, \mathbf{c}) = \begin{cases} \frac{x^{1-\delta}}{1-\delta} \varphi(t, \mathbf{c}), & \delta \in (0, 1) \cup (1, +\infty), \\ \log(x) + \varphi(t, \mathbf{c}), & \delta = 1. \end{cases}$$

Proof. See Appendix A.2. □

Example 3.7. *To analyze the optimal investment strategy, we consider a case in which only two stocks, S_1 and S_2 , are traded in the market, where S_1 is characterized by a positive carbon intensity ($C_1 > 0$) and S_2 has zero carbon intensity ($C_2 = 0$). Hence, equation (3.7) becomes*

$$\pi_1^*(t, c_1) = \frac{\mu_1 - r}{\sigma_1^2 [\delta (1 - \rho^2) + \alpha_1 c_1]} - \frac{\rho (\mu_2 - r)}{\sigma_1 \sigma_2 [\delta (1 - \rho^2) + \alpha_1 c_1]}, \quad (3.8)$$

$$\pi_2^*(t, c_1) = -\frac{\rho (\mu_1 - r)}{\sigma_1 \sigma_2 [\delta (1 - \rho^2) + \alpha_1 c_1]} + \frac{(\delta + \alpha_1 c_1) (\mu_2 - r)}{\delta \sigma_2^2 [\delta (1 - \rho^2) + \alpha_1 c_1]}. \quad (3.9)$$

for every $(t, c_1) \in [0, T] \times \mathbb{R}_+$. When the carbon penalization parameter α is set to zero, we recover the classical myopic Merton solution, namely

$$\begin{aligned} \pi_1^*(t, c_1) &= \frac{1}{\delta} \frac{\mu_1 - r}{\sigma_1^2 (1 - \rho^2)} - \frac{1}{\delta} \frac{\rho (\mu_2 - r)}{\sigma_1 \sigma_2 (1 - \rho^2)}, \\ \pi_2^*(t, c_1) &= -\frac{1}{\delta} \frac{\rho (\mu_1 - r)}{\sigma_1 \sigma_2 (1 - \rho^2)} + \frac{1}{\delta} \frac{\mu_2 - r}{\sigma_2^2 (1 - \rho^2)}. \end{aligned}$$

	S_1	S_2	S_3	S_4
μ	0.25	0.15	0.1	0.08
σ	0.34	0.25	0.2	0.16

Table 3.1: Parameters of stock price process \mathbf{S} .

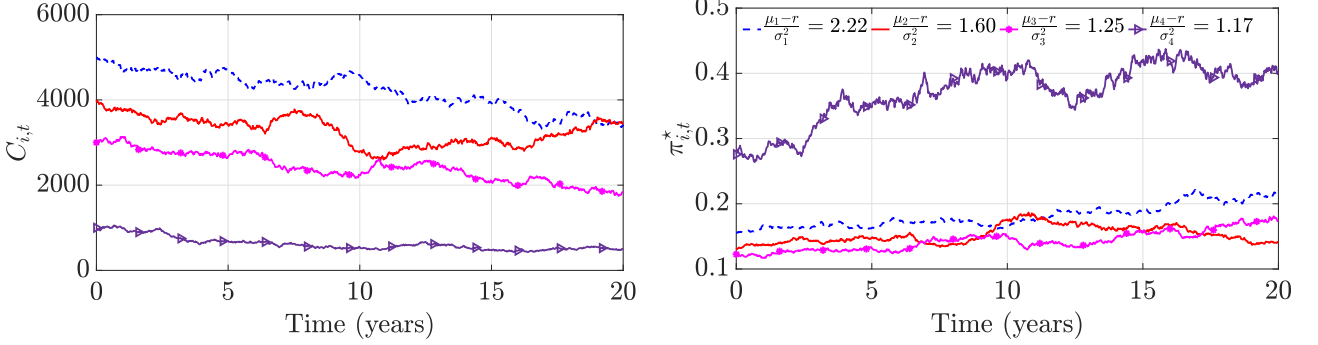


Figure 3.1: The left panel shows the paths of the carbon intensity \mathbf{C} of four stocks, simulated according to the CIR process (see Section 4.2). The right panel shows the corresponding dynamics of the optimal portfolio weights $\boldsymbol{\pi}^*$. Parameters of \mathbf{S} : μ_i and σ_i for every $i = 1, \dots, 4$ are reported in Table 3.1, $\rho_{1,2} = 0.4397$, $\rho_{1,3} = 0.39$, $\rho_{1,4} = 0.3168$, $\rho_{2,3} = 0.2954$, $\rho_{2,4} = 0.3261$ and $\rho_{3,4} = 0.3134$. Parameters of carbon intensity process \mathbf{C} : $C_{0,1} = 2500$, $C_{0,2} = 2000$, $C_{0,3} = 1500$, $C_{0,4} = 500$, $\beta_i = C_{0,i}$, $\kappa_i = 0.05$ and $\lambda_i = 3$, for every $i = 1, \dots, 4$. Investment strategy parameters: $\delta = 1$ (log case), $\alpha_{i,t} = 0.0025$ for every $i = 1, \dots, 4$ and $t \in [0, T]$, with $T = 20$ years.

for every $(t, c_1) \in [0, T] \times \mathbb{R}_+$. In the limiting case, where $\alpha \rightarrow \infty$, $\pi_1^*(t, c_1) = 0$ and $\pi_2^*(t, c_1) = \frac{1}{\delta} \frac{\mu_2 - r}{\sigma_2^2}$, meaning that S_1 is fully divested and the entire risky allocation is shifted to S_2 with zero carbon intensity. It is also interesting to comment on the case in which the correlation ρ between the two stocks is equal to zero. In this case, equations (3.8) and (3.9) become, respectively:

$$\pi_1^*(t, c_1) = \frac{1}{\delta + \alpha_1 c_1} \frac{\mu_1 - r}{\sigma_1^2}, \quad \pi_2^*(t, c_1) = \frac{1}{\delta} \frac{\mu_2 - r}{\sigma_2^2}.$$

In this case, any increase in α leads to a reduction in the exposure to the carbon-intensive asset, while the allocation to the zero-carbon emission asset remains unchanged, resulting in an increase in the exposure to the risk-free asset.

Remark 3.8. To analyze how the proposed carbon penalization mechanism shapes portfolio allocation, we simulate the optimal portfolio weights $\boldsymbol{\pi}^*$ over the entire investment horizon. The results are shown in Figure 3.1, suggesting that our model successfully balances the risk–return trade-off of each stock with its corresponding carbon risk. In particular, stock 4, which maintains the lowest carbon intensity throughout the investment horizon, is consistently assigned the highest weight, reflecting the model’s sensitivity to sustainability criteria. However, the proposed portfolio selection methodology does not reduce to a naive exclusion of carbon intensive assets. Indeed, although stock 1 has the highest carbon intensity, it is assigned higher optimal portfolio weights than stocks 2 and 3 throughout most of the investment horizon. This is justified by the fact that stock 1 exhibits the highest market price of risk, indicating that its financial attractiveness is sufficient to outweigh its carbon risk. This outcome highlights that our penalization mechanism does not rigidly exclude high carbon intensive assets, but instead adjusts allocations based on a balanced evaluation of both environmental and financial attributes.

4 Examples: models for carbon intensities and value functions

The limited data available on asset carbon intensity do not allow us to reliably specify a model for this process. Therefore, in this section, we present several plausible dynamics for the carbon intensity process and, for each case, provide the corresponding characterization of the value function.

4.1 Ornstein-Uhlenbeck process

Although we only have a limited number of data points, which prevents us from properly identifying and calibrating the dynamics of the carbon intensity process, we have observed that these data tend to fluctuate around a stable level. This behavior may be attributed to the fact that a substantial shift in a firm's carbon intensity typically results from a technological shock, a change in production management, or the adoption of a green agenda aimed at increasing carbon consumption – thus leading to a significant decrease in the carbon footprint. In particular, the implementation of a green agenda may even result in net negative emission levels (see Remark 3.3). Hence, a natural choice is to model the dynamics of carbon intensity according to an Ornstein–Uhlenbeck process:

$$dC_{i,t} = \kappa_i (\bar{C}_i - C_{i,t}) dt + \lambda_i dW_{i,t}, \quad C_{i,0} = c_{i,0}, \quad (4.1)$$

where $\bar{C}_i \geq 0$ represents the long-term carbon intensity level, $\kappa_i > 0$ governs the strength of attraction toward the target \bar{C}_i , and λ_i is the volatility of the i -th carbon intensity, for every $i = 1, \dots, d$. Specifically, the target \bar{C}_i reflects internal sustainability goals, regulatory thresholds, industry benchmarks or carbon intensity levels deemed economically feasible by the i -th firm. Furthermore, the corresponding rate of attraction κ_i around the target reflects how strongly the firm reacts to environmental pressures or incentives – such as carbon regulations, investor scrutiny, or reputational concerns – that drive decarbonization efforts over time. $\mathbf{W} = (W_{1,t}, \dots, W_{d,t})^\top$ is a vector of uncorrelated standard \mathbb{F} -Brownian motions independent of \mathbf{Z} , as required in order to satisfy the assumptions made on \mathbf{C} in Section 2. Under this model specification, the infinitesimal generator of \mathbf{C}_t is given by

$$\mathcal{L}^{\mathbf{C}} F(\mathbf{c}) = \sum_{i=1}^d \kappa_i (\bar{C}_i - c_i) \partial_{c_i} F(\mathbf{c}) + \frac{1}{2} \sum_{i=1}^d \lambda_i^2 \partial_{c_i}^2 F(\mathbf{c}), \quad (4.2)$$

for every $F \in \mathcal{C}^2(\mathcal{D})$, with $\mathcal{D} = \mathbb{R}^d$.

Lemma 4.1. *Let $\mathcal{L}^{\mathbf{C}}$ as in equation (4.2) with $\lambda_i > 0$ for every $i \in 1, \dots, d$, and let $\alpha_i(t)$ be Lipschitz continuous functions on $[0, T]$ for every $i \in 1, \dots, d$. Then the problem (3.6) has a unique solution $\varphi(t, \mathbf{c}) \in \mathcal{C}^{1,2}([0, T] \times \mathbb{R}^d) \cap \mathcal{C}([0, T] \times \mathbb{R}^d)$.*

Proof. Note that, under the assumption that $\alpha_i(t)$ is Lipschitz continuous on $[0, T]$ for every $i \in 1, \dots, d$, it holds that $H(t, \mathbf{c})$ and $f(t, \mathbf{c})$ are Lipschitz continuous on $[0, T] \times \mathbb{R}^d$. Hence the result follows from (Krylov, 1996, Theorem 8.2.1, Chapter 8). \square

4.2 Cox-Ingersoll-Ross process

Empirical observations on the released carbon intensities of assets listed in the S&P 500, which we use for the empirical analysis (see Section 5), suggest that these values may remain positive over time. Hence, one could retain the mean-reversion property introduced in equation (4.1) while ensuring that the carbon intensity process remains positive over time. In this case, a suitable modeling choice is to assume that $C_{i,t}$ follows a Cox–Ingersoll–Ross (CIR) process:

$$dC_{i,t} = \kappa_i (\bar{C}_i - C_{i,t}) dt + \lambda_i \sqrt{C_{i,t}} dW_{i,t}, \quad C_{i,0} = c_{i,0},$$

for every $i = 1, \dots, d$, with $C_i, \kappa_i, \lambda_i > 0$. In this case, the infinitesimal generator of \mathbf{C}_t reads as

$$\mathcal{L}^{\mathbf{C}} F(\mathbf{c}) = \sum_{i=1}^d \kappa_i (\bar{C}_i - c_i) \partial_{c_i} F(\mathbf{c}) + \frac{1}{2} \sum_{i=1}^d \lambda_i^2 c_i \partial_{c_i}^2 F(\mathbf{c}), \quad (4.3)$$

for every $f \in \mathcal{C}^2(\mathcal{D})$, with $\mathcal{D} = \mathbb{R}_+^d$.

Lemma 4.2. *Let $\mathcal{L}^{\mathbf{C}}$ as in equation (4.3) and let $\alpha_i(t)$ be Lipschitz continuous functions on $[0, T]$ for every $i \in 1, \dots, d$. Assume that Feller conditions hold, that is, $2\kappa_i \bar{C}_i \geq \lambda_i^2$ for all $i \in \{1, \dots, d\}$. Then the problem (3.6) has a unique solution $\varphi \in \mathcal{C}^{1,2}[0, T] \times \mathbb{R}_+^d \cap \mathcal{C}([0, T] \times \mathbb{R}_+^d)$*

Proof. See Appendix B.1. □

4.3 Exponential of Ornstein-Uhlenbeck process

A possible alternative to the CIR process, which ensures positivity and preserves the mean-reverting structure of carbon intensity, is to use the exponential of the OU process given by equation (4.1). Specifically, its dynamics are given by

$$\frac{dC_{i,t}}{C_{i,t}} = \left[\kappa_i (\bar{C}_i - \ln C_{i,t}) + \frac{\lambda_i^2}{2} \right] dt + \lambda_i dW_{i,t}, \quad C_{i,0} = c_{i,0},$$

for every $i = 1, \dots, d$. Hence,

$$\mathcal{L}^{\mathbf{C}} F(\mathbf{c}) = \sum_{i=1}^d \kappa_i c_i \left[(C_i - \ln c_i) + \frac{\lambda_i^2}{2} \right] \partial_{c_i} F(\mathbf{c}) + \frac{1}{2} \sum_{i=1}^d \lambda_i^2 c_i^2 \partial_{c_i}^2 F(\mathbf{c}), \quad (4.4)$$

for every $F \in \mathcal{C}^2(\mathcal{D})$, with $\mathcal{D} = \mathbb{R}_+^d$.

Lemma 4.3. *Let $\mathcal{L}^{\mathbf{C}}$ as in equation (4.4) with $\lambda_i > 0$ and let $\alpha_i(t)$ be Lipschitz continuous functions on $[0, T]$ for every $i \in 1, \dots, d$. Then the problem (3.6) has a unique solution $\varphi \in \mathcal{C}^{1,2}[0, T] \times \mathbb{R}_+^d \cap \mathcal{C}([0, T] \times \mathbb{R}_+^d)$.*

Proof. The proof of this result follows from the same lines of the proof of Lemma 4.2, see also Appendix B.1. □

4.4 Continuous time finite-state Markov chain

As carbon intensity is not subject to large variations continuously over time, a stylized alternative model would be to assume that \mathbf{C}_t is piecewise constant and consider only consistent fluctuations. In this case, one could model \mathbf{C}_t as a continuous time finite state Markov chain, with K possible states and state space $\mathcal{D} = \{\mathbf{a}_1, \dots, \mathbf{a}_K\}$ and $\mathbf{a}_k \in \mathbb{R}^d$ for $k \in \{1, \dots, K\}$. We denote by $Q = (q_{k,l})_{k,l \in \{1, \dots, K\}}$ the infinitesimal generator of \mathbf{C} , with $q_{k,l} \geq 0$ and $q_{k,k} = -\sum_{l \neq k} q_{k,l}$, and let $\Pi = (\Pi_1, \dots, \Pi_K)$ be its initial distribution. Hence, the infinitesimal generator of \mathbf{C} is given by

$$\mathcal{L}^{\mathbf{C}} F(\mathbf{a}_l) = \sum_{k \neq l} q_{k,l} F(\mathbf{a}_k),$$

for every function $F : \mathcal{D} \rightarrow \mathbb{R}$.

Lemma 4.4. Let $\alpha_i(t)$ be continuous functions on $[0, T]$ for every $i = 1, \dots, d$. Then, $\varphi_k(t) := \varphi(t, \mathbf{a}_k) \in \mathcal{C}^1([0, T])$ are the unique solutions to the system of ODEs

$$\partial_t \varphi_k(t) + \sum_{k \neq l} q_{k,l} \varphi_l(t) + H_k(t) \varphi_k(t) = f_k(t), \quad (4.5)$$

with terminal conditions $\varphi_k(T) = \mathbb{1}_{\{\delta \in (0,1) \cup (1,+\infty)\}}$ for all $k \in \{1, \dots, K\}$, where $H_k(t) := H(t, \mathbf{a}_k)$ and $f_k(t) := f(t, \mathbf{a}_k)$.

Proof. Equation (4.5) defines a system of linear ODEs. The result then follows from (Teschl, 2012, Theorem 3.9). \square

5 Empirical findings

The empirical implementation of the model is based on a selection of $d = 34$ stocks from the S&P500 index. We calibrate the model in equation (2.1) using daily closing prices of these stocks over the period from January 1, 2015 to December 31, 2024, sourced from Morningstar database. Based on the calibrated market parameters, we analyze the behavior of the optimal carbon penalized strategy $\boldsymbol{\pi}^*$ at $t = 0$. For each of the selected stocks, the corresponding value of carbon intensity at $t = 0$, denoted by $c_{i,0}$ for every $i = 1, \dots, d$, is given by the most recently available observation. These values correspond to the data released on December 31, 2024, and serve as the starting point for the carbon intensity processes, namely $C_{i,0} = c_{i,0}$ for every $i = 1, \dots, d$. We recall that a firm's carbon intensity is defined as the ratio between the total GHG emissions in metric tonnes of CO₂ and total revenues (in USD millions). We consider the definition of carbon intensity that includes, in the numerator, only Scope 1 and Scope 2 GHG emissions. Moreover, we exclude Scope 3 emissions, as they are notoriously difficult to assess and subject to significant methodological uncertainty, as highlighted by Anquetin et al. (2022).⁽³⁾ We take a constant and homogeneous penalty for each stock in the portfolio, that is $\alpha_i(t) = \alpha$ for every $t \in [0, T]$, and every $i = 1, \dots, d$. Scatter plots in Figure 5.1 illustrate the relationship between the carbon intensity $C_{i,0}$ on the x -axis and the corresponding optimal portfolio weight $\pi_{i,0}^*$ on the y -axis of the i -th stock for every $i = 1, \dots, d$, for different levels of the fund manager's risk aversion δ and carbon penalization α . Each panel corresponds to a specific combination of $\delta \in \{0.7, 1, 3\}$ and $\alpha \in \{0, 0.0075, 0.015\}$, allowing for a comparative analysis of how increasing values of carbon aversion affect the allocation strategy. The results clearly show that, as the carbon penalization α increases, the optimal weights of carbon-intensive stocks decrease in absolute value, regardless of the level of the risk aversion parameter δ . Increasing values of δ do not modify the impact of carbon penalization; instead, they reduce the strategy's exposure to risky assets, which in turn leads to lower leverage in the optimal portfolio. This is also confirmed by figure 5.2, which illustrates the relationship between carbon penalization α and the corresponding optimal portfolio allocation to bank account $\pi^{*,0}$. When $\alpha = 0$, or takes small values, the portfolio may exhibit leverage, but only in case of low risk aversion or logarithmic preferences; for higher levels of risk aversion (e.g., $\delta = 3$), no leverage is observed. As α increases, the investment in the bank account rises, implying that the overall exposure to risky assets $\boldsymbol{\pi}^* \mathbf{1}$ decreases, regardless of the level of the risk aversion parameters δ . In the limit, for very large penalization values, $\pi^{*,0}$ tends to 1 implying that the entire fund wealth is invested in the bank account. To further quantify the impact of α

⁽³⁾Scope 1 refers to direct greenhouse gas emissions from sources owned or controlled by the company; Scope 2 includes indirect emissions from the generation of purchased electricity, steam, heating, and cooling; Scope 3 covers all other indirect emissions across the company's value chain, including those related to purchased goods and services, business travel, waste disposal, and product use.

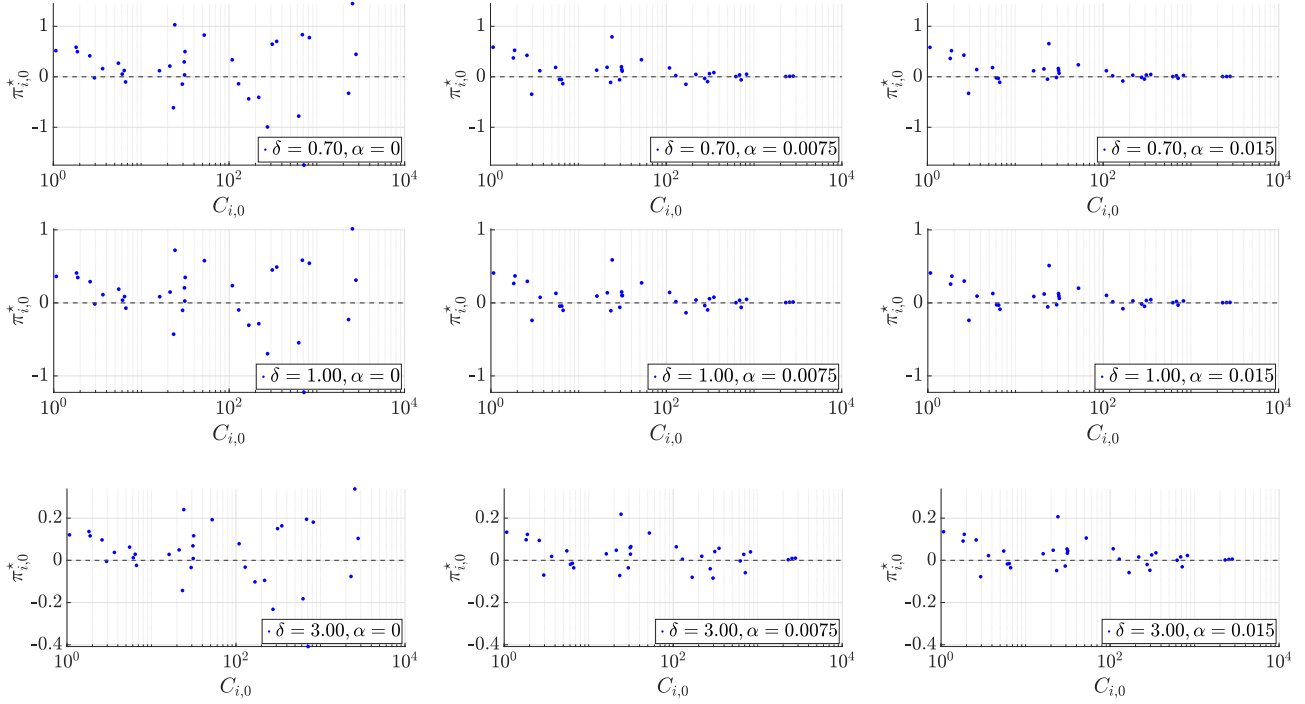


Figure 5.1: Scatter plots displaying the carbon intensity of the i -th stock (x -axis on logarithmic scale) and the optimal portfolio weights (y -axis) for different levels of δ and α .

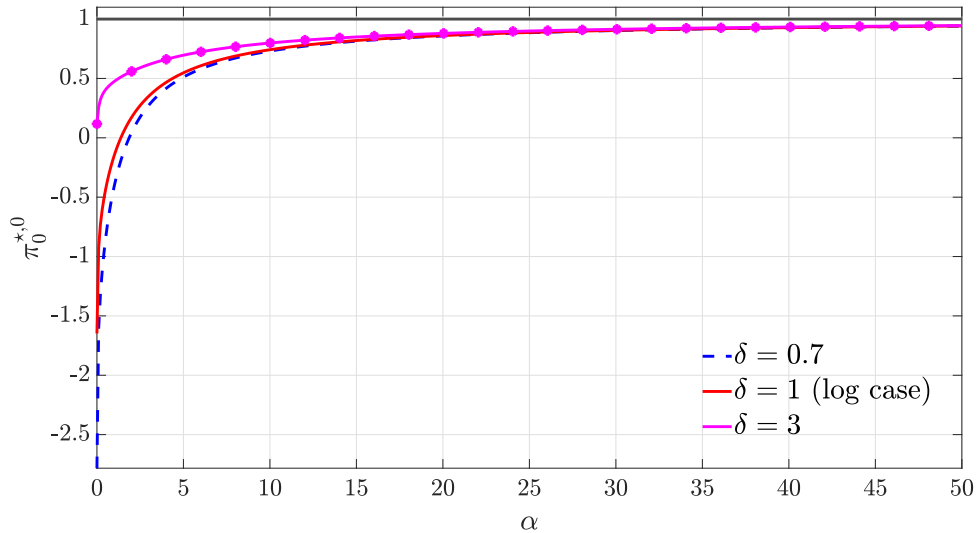


Figure 5.2: Optimal portfolio weight in the bank account, $\pi_0^{0,*} = 1 - \sum_{i=1}^d \pi_{i,0}^*$, as a function of the carbon penalization α , for different levels of market risk aversion δ .

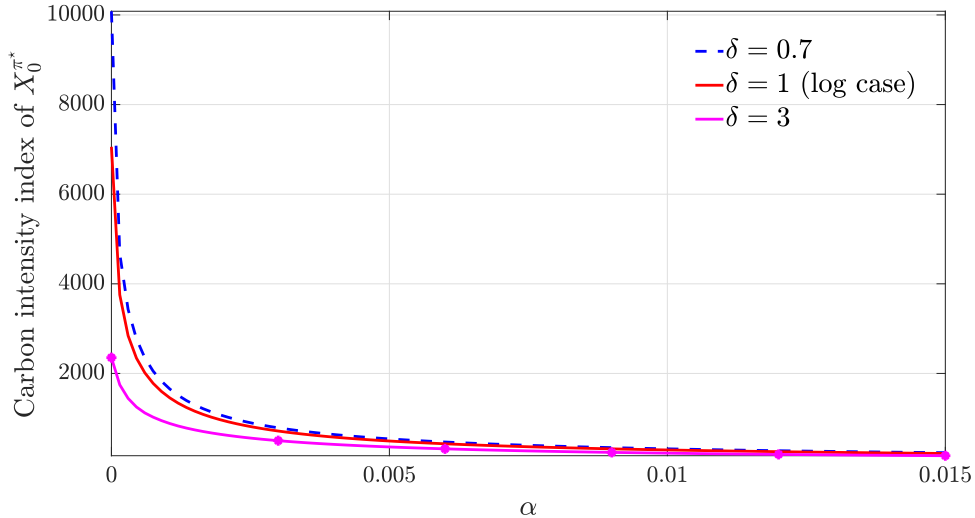


Figure 5.3: Carbon intensity index of the optimal portfolio X^{π^*} at $t = 0$ as a function of carbon penalization α , for different levels of market risk aversion δ . The portfolio carbon intensity index is computed as $\sum_{i=1}^d |\pi_{i,0}^*| C_{i,0}$.

on the environmental sustainability of the investment strategy, Figure 5.3 reports the total carbon intensity of the optimal portfolio as a function of α , for different levels of δ . These plots confirm that the portfolio's carbon intensity decreases as α increases and that a very small penalization is enough to considerably diminish the carbon intensity index of the portfolio. Moreover, consistent with the results shown in Figure 5.1, lower levels of δ lead the strategy to take on greater exposure to risky assets and, for a given α , result in a smaller reduction in carbon intensity.

6 Risk-minimizing strategies for unit linked policies under carbon risk

In the sequel, we take the point of view of an insurance company who proposes to its clients unit linked life insurance contracts with a green footprint and seeks to hedge their payoffs. As usual in this type of life insurance policy, the value is linked to the performance of an underlying fund, and its maturity relates to the policyholder's remaining lifetime. In particular, in this case, we consider a fund which has been appropriately optimized using a criterion sensitive to environmental factors, with a particular focus on carbon intensity, as described in Section 3. Consequently, the insurer faces exposure to financial, carbon, and mortality risks. Since the carbon emissions of the firms and mortality risk do not correspond to tradeable assets, the underlying combined financial/insurance market is incomplete. Hence, the insurance company is unable to replicate the payoff of the policy via a self financing strategy. Part of the risk related to this contract remains unhedgeable, and generates a loss that the insurer would like to properly *minimize*. In this paper, we follow a quadratic approach and determine the strategies that minimize the tracking error in L^2 -sense.

6.1 A market for green unit linked contracts

We consider the financial market of Section 2, and extend it by including a group of individuals to be insured. To do this, we consider a probability space $(\Omega^I, \mathcal{H}, \mathbb{P}^I)$. We consider a set of ℓ independent individuals of age (a_1, \dots, a_ℓ) , and let $(\tau_1, \dots, \tau_\ell)$ be nonnegative random variables representing their remaining lifetime. We assume that $(\tau_1, \dots, \tau_\ell)$ are independent, doubly-stochastic random times

having hazard rate processes γ_t^i such that for all $t_1, t_2, \dots, t_\ell \geq 0$,

$$\mathbb{P}^I(\tau_1 > t_1, \dots, \tau_\ell > t_\ell) = \prod_{i=1}^{\ell} \mathbb{E}^I \left[\exp \left(- \int_0^{t_i} \gamma_s^i ds \right) \right],$$

where, \mathbb{E}^I denotes the expectation under the probability measure \mathbb{P}^I . We set $H_t^i := \mathbb{1}_{\{\tau_i \leq t\}}$, for every $t \geq 0$, and define the filtration $\mathbb{H} := \{\mathcal{H}_t\}_{t \geq 0}$ generated by the vector process (H^1, \dots, H^ℓ) , i.e.,

$$\mathcal{H}_t := \sigma\{H_s^i, 0 \leq s \leq t, i = 1, \dots, \ell\}, \quad \text{for all } t \geq 0.$$

In the sequel, we assume that $\mathbb{E}^I \left[\int_0^T \gamma_s^i ds \right] < \infty$, then $\left\{ H_t^i - \int_0^{t \wedge \tau_i} \gamma_s^i ds, t \geq 0 \right\}$, is a $(\mathbb{H}, \mathbb{P}^I)$ -martingale. Note that we can interpret \mathbb{P}^I as the probability measure corresponding to the mortality table used by the insurance company.

Next, we define the combined financial-insurance market, which is the natural framework for unit linked life insurance contracts. We consider the probability space $(\Omega, \mathcal{G}, \mathbb{P})$ with the filtration \mathbb{G} as our mathematical environment, where $\Omega = \Omega^M \times \Omega^I$, $\mathcal{G} = \mathcal{F} \vee \mathcal{H}$, $\mathbb{P} = \mathbb{P}^M \times \mathbb{P}^I$ and $\mathbb{G} = \{\mathcal{G}_t\}_{t \in [0, T]}$ given by $\mathcal{G}_t = \mathcal{F}_t \vee \mathcal{H}_t$, for every $t \in [0, T]$. Note that, according to this construction, the insurance market is independent of the a priori given financial market. For the case where the financial and the insurance market are correlated, we refer to Ceci et al. (2017), where also partial information on the mortality intensity is assumed.

We assume that the insurance company issues green unit linked life insurance policies, for a group of individuals with mortality intensities γ^i . Under this type of life insurance contract the value of the benefit depends on the investment fund, optimized in Section 3, and the time of payment depends on the death time of the individual. In this paper, we develop hedging strategies for two types of unit linked contracts, namely the Pure Endowment and the Term Insurance. Benefits of these contracts are illustrated below in Sections 6.3 and 6.4.

6.2 The quadratic hedging criterion

In this section, we deal with the combined financial-insurance market which consists of $(d+1)$ -tradeable assets and a unit linked contract. This market is incomplete for two reasons. First, in view of equation (6.2), the variations of carbon emission levels \mathbf{C} which appear in an integrated form, directly affect the payoff structure. This risk cannot be hedged by trading in \mathbf{S} . Second, mortality risk cannot be covered through market investments.

Remark 6.1. *Partial hedging of mortality risk can be obtained by investing in, e.g., longevity bonds. However, we opt against introducing these investment opportunities for the following reasons. Longevity bonds are not widely traded, and the market for them is extremely illiquid. This lack of depth creates pricing uncertainty and high transaction costs, which undermines their usefulness in dynamic hedging strategies. In practice, it becomes difficult to adjust or unwind positions, making them unreliable for continuous risk management in a stochastic setting. Moreover, longevity bonds are typically linked to general population mortality indices, such as national life tables. However, insurance companies often underwrite lives from more specific, healthier subsets (e.g., individuals with medical underwriting or higher socio-economic status). This mismatch creates basis risk, meaning that changes in the bond's value may not accurately reflect the longevity risk exposure of the insurer's actual portfolio.*

Because of market incompleteness, every equivalent probability measure \mathbb{Q} has the following density

$L^{\mathbb{Q}} = \{L_t^{\mathbb{Q}}\}_{t \in [0, T]}$, with

$$L_t^{\mathbb{Q}} = \frac{d\mathbb{Q}}{d\mathbb{P}} \Big|_{\mathcal{G}_t} = \mathcal{E} \left(- \int_0^t \boldsymbol{\theta}_s^\top d\mathbf{Z}_s + \int_0^t \psi_s^{\mathbb{Q}} d\mathbf{W}_s + \sum_{i=1}^{\ell} \int_0^t \varphi_s^{i, \mathbb{Q}} (dH_s^i - \gamma_s^i ds) \right), \quad t \in [0, T],$$

where

$$\boldsymbol{\theta}_t = \boldsymbol{\Sigma}^{-1} (\boldsymbol{\mu} - \mathbf{1}r),$$

$\psi^{\mathbb{Q}} = \{\psi_t^{\mathbb{Q}}\}_{t \in [0, T]}$ and $\varphi^{i, \mathbb{Q}} = \{\varphi_t^{i, \mathbb{Q}}\}_{t \in [0, T]}$ are \mathbb{G} -predictable processes, $\varphi_t^{i, \mathbb{Q}} > -1$ for all t , such that $L^{\mathbb{Q}}$ is a (\mathbb{G}, \mathbb{P}) -martingale with expected value equal to 1. The mortality intensity, under the probability measure \mathbb{Q} , is given by $\gamma^{i, \mathbb{Q}} = (1 + \varphi^{i, \mathbb{Q}})\gamma^i$. Here, $\mathcal{E}(Y)$ denotes the Doléans-Dade exponential of a (\mathbb{G}, \mathbb{P}) -semimartingale Y . In view of the fact that \mathbb{P}^I is the probability measure used by the insurance company to estimate the mortality of the insured individual (i.e., it corresponds to a specific mortality table used by the insurance company), we may also assume that it already incorporates the mortality premium. Therefore, in the following, we assume that $\varphi^{i, \mathbb{Q}} = 0$. Note that, because of independence between the measure \mathbb{P}^I and the financial market, this assumption does not affect the computation of the hedging strategy from a technical perspective. In particular, what changes is that $\gamma^{i, \mathbb{Q}}$ would replace γ^i .

The choice $\Psi_t^{\mathbb{Q}} = 0$, for every $t \in [0, T]$, corresponds to the so-called *minimal martingale measure* (see, e.g., Föllmer and Schweizer (2010)), denoted by \mathbb{Q}^* , whose density process $L = \{L_t\}_{t \in [0, T]}$ is defined by

$$L_t = \frac{d\mathbb{Q}^*}{d\mathbb{P}} \Big|_{\mathcal{G}_t} = \mathcal{E} \left(- \int_0^t \boldsymbol{\theta}_s^\top d\mathbf{Z}_s \right), \quad t \in [0, T].$$

Note that L is a square-integrable (\mathbb{G}, \mathbb{P}) -martingale. Girsanov theorem implies that the process $\widehat{\mathbf{Z}} = \{\widehat{\mathbf{Z}}_t\}_{t \in [0, T]}$, given by

$$\widehat{\mathbf{Z}}_t = \mathbf{Z}_t + \int_0^t \boldsymbol{\theta}_s ds, \quad t \in [0, T],$$

is a $(\mathbb{G}, \mathbb{Q}^*)$ -Brownian motion. It is also worth noting that, in view of the independence between the financial market and the individuals lifetime, we can define the probability measure \mathbb{Q}^M , equivalent to \mathbb{P}^M , with the density

$$L_t^M = \frac{d\mathbb{Q}^M}{d\mathbb{P}^M} \Big|_{\mathcal{F}_t} = \mathcal{E} \left(- \int_0^t \boldsymbol{\theta}_s^\top d\mathbf{Z}_s \right), \quad t \in [0, T].$$

Hence, we also get that $\widehat{\mathbf{Z}}$ is a $(\mathbb{F}, \mathbb{Q}^M)$ -Brownian motion and the vector of discounted risky asset price processes $\widetilde{\mathbf{S}} = \{\widetilde{\mathbf{S}}_t\}_{t \in [0, T]}$, with $\widetilde{\mathbf{S}}_t := e^{-rt}\mathbf{S}_t$, is an $(\mathbb{F}, \mathbb{Q}^M)$ -martingale.

6.3 Hedging of a Pure Endowment

To begin, we consider a Pure Endowment Insurance contract with maturity of T years, whose payoff is

$$\phi(X_T^{\pi^*}) \mathbf{1}_{\{\tau > T\}}, \quad (6.1)$$

where X^{π^*} is given by

$$\frac{dX_t^{\pi^*}}{X_t^{\pi^*}} = \left[r + \boldsymbol{\pi}_t^{*, \top} (\boldsymbol{\mu} - \mathbf{1}r) \right] dt + \boldsymbol{\pi}_t^{*, \top} \boldsymbol{\Sigma} d\mathbf{Z}_t, \quad X_0^{\pi^*} = x_0, \quad (6.2)$$

with $\boldsymbol{\pi}_t^* = \boldsymbol{\pi}^*(t, \mathbf{C}_t)$ as in equation (3.7). X^{π^*} is the value of the optimized fund (see Theorem 3.6). The function $\phi : \mathbb{R}^+ \rightarrow \mathbb{R}^+$ defines the benefit structure that is, $\phi(X_T^{\pi^*})$ provides the amount to be

paid at maturity T , if the policyholder is still alive at time T . The payoff of the Pure Endowment portfolio is then given by

$$G^{PE} = \sum_{i=1}^{\ell} \phi^i(X_T^{\pi^*}) \mathbf{1}_{\{\tau_i > T\}},$$

for functions $\phi^i : \mathbb{R}^+ \rightarrow \mathbb{R}^+$. We assume that $\phi^i(X_T^{\pi^*}) \in L^2(\mathcal{F}_T, \mathbb{P})$, and hence $G^{PE} \in L^2(\mathcal{G}_T, \mathbb{P})$. A typical example of benefit is $\phi(x) = \min(\max(x, k), K)$, which includes a minimum guarantee $k > 0$ and a maximum amount $K > 0$ for the policy holder. The insurance company seeks to hedge a Pure Endowment contract whose payoff is given by (6.1). Because of market incompleteness, we adopt the local risk-minimization approach to determine a hedging strategy that replicates the payoff at maturity and minimizes the strategy costs in a suitable way. The first step is to introduce the class of all admissible hedging strategies.

Definition 6.2. *The space $\Theta^{\mathbf{S}}$ consists of all \mathbb{R}^d -valued \mathbb{G} -predictable processes $\boldsymbol{\eta} = \{\boldsymbol{\eta}_t\}_{t \in [0, T]}$ satisfying the following integrability condition:*

$$\mathbb{E}^{\mathbb{P}} \left[\int_0^T \|\boldsymbol{\eta}_u^{\top} \boldsymbol{\Sigma} \text{diag}(\tilde{\mathbf{S}}_u)\|^2 + |\boldsymbol{\eta}_u^{\top} \text{diag}(\tilde{\mathbf{S}}_u)(\boldsymbol{\mu} - \mathbf{1}r)| du \right] < +\infty.$$

Definition 6.3. *An admissible strategy is a pair $(\boldsymbol{\eta}, \zeta)$, where $\boldsymbol{\eta} \in \Theta^{\mathbf{S}}$ and $\zeta = \{\zeta_t\}_{t \in [0, T]}$ is a \mathbb{R} -valued \mathbb{G} -adapted process such that the associated discounted value process $V(\boldsymbol{\eta}, \zeta) = \boldsymbol{\eta}^{\top} \tilde{\mathbf{S}} + \zeta$ is right-continuous and square-integrable, i.e., $V_t(\boldsymbol{\eta}, \zeta) \in L^2(\mathcal{G}_t, \mathbb{P})$ for every $t \in [0, T]$.*

Here, the processes $\boldsymbol{\eta}$ and ζ represent, respectively, the units of all risky and riskless assets held in the portfolio. For any admissible hedging strategy $(\boldsymbol{\eta}, \zeta)$, we can define the associated *cost process* $C(\boldsymbol{\eta}, \zeta) = \{C_t(\boldsymbol{\eta}, \zeta)\}_{t \in [0, T]}$, which is the \mathbb{R} -valued \mathbb{G} -adapted process given by

$$C_t(\boldsymbol{\eta}, \zeta) = V_t(\boldsymbol{\eta}, \zeta) - \int_0^t \boldsymbol{\eta}_u^{\top} d\tilde{\mathbf{S}}_u, \quad t \in [0, T],$$

Although admissible strategies that replicate the payoff at maturity, i.e., $V_T(\boldsymbol{\eta}, \zeta) = G^{PE}$, will in general not be self-financing, it turns out that good admissible strategies are self-financing *on average* in the following sense.

Definition 6.4. *An admissible strategy $(\boldsymbol{\eta}, \zeta)$ is called mean-self-financing if the associated cost process $C(\boldsymbol{\eta}, \zeta)$ is a (\mathbb{G}, \mathbb{P}) -martingale.*

Following the idea of Schweizer (2001), we now introduce the concept of pseudo-optimal strategy in this framework.⁽⁴⁾

Definition 6.5. *Let $G^{PE} \in L^2(\mathcal{G}_T, \mathbb{P})$ be the payoff of a Pure Endowment. An admissible strategy $(\boldsymbol{\eta}, \zeta)$, such that $V_T(\boldsymbol{\eta}, \zeta) = G^{PE}$ \mathbb{P} -a.s., is called pseudo-optimal for G^{PE} if and only if $(\boldsymbol{\eta}, \zeta)$ is mean-self-financing and the (\mathbb{G}, \mathbb{P}) -martingale $C(\boldsymbol{\eta}, \zeta)$ is strongly orthogonal to the \mathbb{P} -martingale part of $\tilde{\mathbf{S}}$.*

Note that, in our setup, to be strongly orthogonal to the martingale part of $\tilde{\mathbf{S}}$ is equivalent to be strongly orthogonal to \mathbf{Z} . The key result for finding pseudo-optimal strategies is the Föllmer–Schweizer decomposition.

⁽⁴⁾We resort to the definition and the computation of pseudo-optimal strategies, although they are technically different from locally-risk minimizing strategies. The main reason is that pseudo-optimal strategies are easier to characterise according to the procedure explained below, and under general modeling assumptions they coincide with locally-risk minimizing strategies. We refer to Schweizer (2001) for more details.

Definition 6.6. A random variable $G \in L^2(\mathcal{G}_T, \mathbb{P})$ admits the Föllmer–Schweizer decomposition with respect to $\tilde{\mathbf{S}}$ if there exists a random variable $G_0 \in L^2(\mathcal{G}_0, \mathbb{P})$, a process $\boldsymbol{\eta}^G \in \Theta^{\mathbf{S}}$, and a square-integrable (\mathbb{G}, \mathbb{P}) -martingale $O = \{O_t\}_{t \in [0, T]}$ strongly orthogonal to \mathbf{Z} with $O_0 = 0$, such that

$$G = G_0 + \int_0^T \boldsymbol{\eta}_t^G d\tilde{\mathbf{S}}_t + O_T, \quad \mathbb{P}\text{-a.s.} \quad (6.3)$$

Proposition 6.7. A Pure Endowment Insurance contingent claim $G^{PE} \in L^2(\mathcal{G}_T, \mathbb{P})$ admits a unique pseudo-optimal strategy $(\boldsymbol{\eta}^*, \zeta^*)$, with $V_T(\boldsymbol{\eta}^*, \zeta^*) = G^{PE}$ \mathbb{P} -a.s., if and only if G^{PE} admits the decomposition (6.3). The strategy $(\boldsymbol{\eta}^*, \zeta^*)$ is explicitly given by

$$\boldsymbol{\eta}_t^* = \boldsymbol{\eta}_t^{G^{PE}}, \quad t \in [0, T],$$

where $\boldsymbol{\eta}_t^{G^{PE}}$ is the integrand in the Föllmer–Schweizer decomposition of G^{PE} , with minimal cost

$$C_t(\boldsymbol{\eta}^*, \zeta^*) = G_0 + O_t, \quad t \in [0, T],$$

and the corresponding discounted value process is

$$V_t(\boldsymbol{\eta}^*, \zeta^*) = G_0 + \int_0^t \boldsymbol{\eta}_u^{G^{PE}, \top} d\tilde{\mathbf{S}}_u + O_t, \quad t \in [0, T],$$

so that $\zeta_t^* = V_t(\boldsymbol{\eta}^*, \zeta^*) - \boldsymbol{\eta}_t^{*, \top} \tilde{\mathbf{S}}_t$, for every $t \in [0, T]$.

According to the local risk-minimization approach, when the risky asset price processes are continuous and satisfies the structure condition⁽⁵⁾, the Föllmer–Schweizer decomposition of a given square integrable random variable can be computed by switching to the minimal martingale measure, and considering the corresponding Galtchouk–Kunita–Watanabe decomposition. We assume that, for every $i = 1, \dots, \ell$, $\phi^i(X_T^{\pi^*}) \in L^2(\mathcal{F}_T, \mathbb{P})$ admits the Föllmer–Schweizer decomposition with respect to $\tilde{\mathbf{S}}$ and \mathbb{F} , i.e.,

$$\phi^i(X_T^{\pi^*}) = U_0^i + \int_0^T \boldsymbol{\beta}_t^{i, \top} d\mathbf{S}_t + A_T^i \quad \mathbb{P}\text{-a.s.},$$

where $U_0^i \in L^2(\mathcal{F}_0, \mathbb{P})$, $\boldsymbol{\beta}^i \in \Theta(\mathbb{F})$, and $A^i = \{A_t^i\}_{t \in [0, T]}$ is a square-integrable (\mathbb{F}, \mathbb{P}) -martingale strongly orthogonal to the \mathbb{P} -martingale part of $\tilde{\mathbf{S}}$ with $A_0 = 0$. Taking the conditional expectation with respect to \mathcal{G}_t under the minimal martingale measure \mathbb{Q}^* , we get

$$\begin{aligned} \mathbb{E}^{\mathbb{Q}^*} [G^{PE} \mid \mathcal{G}_t] &= \mathbb{E}^{\mathbb{Q}^*} \left[\sum_{i=1}^{\ell} \phi^i(X_T^{\pi^*}) \mathbf{1}_{\{\tau_i > T\}} \mid \mathcal{G}_t \right] \\ &= \sum_{i=1}^{\ell} \mathbb{E}^{\mathbb{Q}^M} \left[\phi^i(X_T^{\pi^*}) \mid \mathcal{F}_t \right] \mathbf{1}_{\{\tau_i > t\}} \mathbb{E}^{\mathbb{P}^I} \left[e^{-\int_t^T \gamma_s^i ds} \right], \quad t \in [0, T], \end{aligned} \quad (6.4)$$

where we used the independence between the financial market and the insured individual, and the fact that $\mathbb{Q}^* = \mathbb{Q}^M \times \mathbb{P}^I$. We now define, for each $i = 1, \dots, \ell$, the processes $B^i = \{B_t^i\}_{t \in [0, T]}$ and

⁽⁵⁾A process $Y = (Y_t)_{t \in [0, T]}$ is said to satisfy the structure condition if it is a semimartingale that admits the following decomposition:

$$Y_t = Y_0 + M_t + \int_0^t \alpha_u d[M]_u,$$

for all $t \in [0, T]$.

$U^i = \{U_t^i\}_{t \in [0, T]}$ as follows:

$$B_t^i := \mathbf{1}_{\{\tau_i > t\}} \mathbb{E}^{\mathbb{P}^I} \left[e^{-\int_t^T \gamma_s^i ds} \right], \quad (6.5)$$

$$U_t^i := \mathbb{E}^{\mathbb{Q}^M} [\phi^i(X_T^{\pi^*}) \mid \mathcal{F}_t] \mathbb{E}^{\mathbb{Q}^M} \left[U_0^i + \int_0^T \beta_u^{i, \top} d\mathbf{S}_u + A_t^i \mid \mathcal{F}_t \right] = U_0^i + \int_0^t \beta_u^{i, \top} d\mathbf{S}_u + A_t^i, \quad (6.6)$$

in view of the decomposition of $\phi^i(X_T^{\pi^*})$ and the martingale-preserving property of the minimal martingale measure. Note that, since, for every $i = 1, \dots, \ell$, $\{B_t^i\}_{t \in [0, T]}$ is a $(\mathbb{H}, \mathbb{P}^I)$ -square-integrable martingale, we can use the martingale representation theorem to write B^i in a more convenient way. In particular, by (Jacod and Shiryaev, 1987, Chapter 3, Theorem 4.37), there exist $(\mathbb{H}, \mathbb{P}^I)$ -predictable processes $\xi^i = \{\xi_t^i\}_{t \in [0, T]}$ such that

$$B_t^i = B_0^i + \int_0^t \xi_u^i (dH_u^i - (1 - H_u^i) \gamma_u^i du), \quad (6.7)$$

with $B_0^i = \mathbb{E}^{\mathbb{P}^I} [1 - H_T^i] = 1 - \mathbb{E}^{\mathbb{P}^I} \left[\int_0^T (1 - H_t^i) \gamma_t^i dt \right]$.

Proposition 6.8. *The insurance portfolio $G^{PE} = \sum_{i=1}^{\ell} \phi^i(X_T^{\pi^*}) \mathbf{1}_{\{\tau_i > T\}}$ admits the Föllmer–Schweizer decomposition given by*

$$G^{PE} = G_0 + \int_0^T \sum_{i=1}^{\ell} B_{s-}^i \beta_s^{i, \top} d\mathbf{S}_s + O_T \quad \mathbb{Q}^* \text{-a.s.},$$

where

$$G_0 = \sum_{i=1}^{\ell} \mathbb{E}^{\mathbb{Q}^M} [\phi^i(X_T^{\pi^*}) \mid \mathcal{F}_0] \mathbb{P}^I(\mathbf{1}_{\{\tau_i > T\}}) = \sum_{i=1}^{\ell} U_0^i \mathbb{E}^{\mathbb{P}^I} \left[e^{-\int_0^T \gamma_s^i ds} \right],$$

and

$$O_t = \int_0^t \sum_{i=1}^{\ell} B_{s-}^i dA_s^i + \int_0^t \sum_{i=1}^{\ell} U_{s-}^i \xi_s^i (dH_s^i - (1 - H_s^i) \gamma_s^i ds), \quad t \in [0, T],$$

where ξ^i is the $(\mathbb{G}, \mathbb{P}^M)$ -predictable process from the martingale representation of B^i (see equation (6.7)). Then, the \mathbb{G} -pseudo-optimal strategy $(\boldsymbol{\eta}^*, \zeta^*)$ is given by

$$\boldsymbol{\eta}_t^* = \sum_{i=1}^{\ell} B_{t-}^i \beta_t^i, \quad \zeta_t^* = V_t(\boldsymbol{\eta}^*, \zeta^*) - \sum_{i=1}^{\ell} B_t \beta_t^{i, \top} \mathbf{S}_t, \quad t \in [0, T],$$

and the optimal value process $V(\boldsymbol{\eta}^*, \zeta^*)$ is

$$V_t(\boldsymbol{\eta}^*, \zeta^*) = G_0 + \int_0^t \sum_{i=1}^{\ell} B_{r-}^i \beta_r^{i, \top} d\mathbf{S}_r + O_t, \quad t \in [0, T].$$

Proof. See Appendix C.1. □

In the sequel, we provide a characterization of the processes $\boldsymbol{\beta}$ and B . We begin with $\boldsymbol{\beta}$, which can be obtained via the proposition below.

Proposition 6.9. *Let $\phi^i(X_T^{\pi^*}) \in L^2(\mathcal{F}_T, \mathbb{P}^M)$ be a contingent claim, and let $\tilde{\varphi}^i = (\tilde{\boldsymbol{\beta}}^i, \tilde{\zeta}^i)$ be the associated pseudo-optimal strategy with respect to \mathbb{F} , for every $i = 1, \dots, \ell$. Then, the optimal discounted value process $\{V_t(\tilde{\varphi}^i)\}_{t \in [0, T]}$ is given by*

$$V_t(\tilde{\varphi}^i) = \mathbb{E}^{\mathbb{Q}^M} [\phi^i(X_T^{\pi^*}) \mid \mathcal{F}_t],$$

and we have that $\beta_t^i = \frac{\partial F^i}{\partial x}(t, X_t^{\pi^*}, \mathbf{C}_t)\pi_t^*$ for every $t \in [0, T]$, where the function $F^i(t, x, \mathbf{c})$ is unique the solution of the backward equation

$$\begin{cases} \frac{\partial F^i}{\partial x}(t, x, \mathbf{c})xr + \frac{\partial^2 F^i}{\partial x^2}(t, x, \mathbf{c})x^2\pi^\top \Sigma \Sigma^\top \pi + \mathcal{L}^{\mathbf{C}}F^i(t, x, \mathbf{c}) = 0, & (t, x, \mathbf{c}) \in [0, T] \times \mathbb{R}_+ \times \mathcal{D}, \\ F^i(T, x, \mathbf{c}) = \phi^i(x), & (x, \mathbf{c}) \in \mathbb{R}_+ \times \mathcal{D}, \end{cases} \quad (6.8)$$

for every $i = 1, \dots, l$.

Proof. See Appendix C.2. □

6.4 Hedging of Term Insurance

Our second example is the Term Insurance contract, which is a mortality benefit that pays the agreed amount to the beneficiary at the time of insured death, provided that it occurs before maturity T . Its payoff is given by

$$\psi(\tau, X_\tau^{\pi^*})\mathbf{1}_{\{\tau \leq T\}},$$

for some function $\psi : [0, T] \times \mathbb{R}^+ \rightarrow \mathbb{R}^+$ such that $\phi^{TI}(\tau, X_\tau^{\pi^*}) \in L^2(\mathcal{F}_T, \mathbb{P})$.⁽⁶⁾ Hence, the corresponding payoff is

$$\phi(X_T^{\pi^*})\mathbf{1}_{\{\tau > T\}} + \psi(\tau, X_\tau^{\pi^*})\mathbf{1}_{\{\tau \leq T\}}.$$

For a portfolio of Term Insurance contracts, the payoff is given by

$$G^{TI} = \sum_{i=1}^{\ell} \psi^i(\tau_i, X_{\tau_i}^{\pi^*})\mathbf{1}_{\{\tau_i > T\}} = \int_0^T \sum_{i=1}^{\ell} \psi^i(s, X_s^{\pi^*})dH_s^i,$$

for functions $\psi^i : [0, T] \times \mathbb{R}^+ \rightarrow \mathbb{R}^+$ such that $\psi^i(\tau, X_\tau^{\pi^*}) \in L^2(\mathcal{F}_T, \mathbb{P})$. Moreover, $G^{TI} \in L^2(\mathcal{G}_T, \mathbb{P}^M)$. In this section, we aim to compute the pseudo-optimal strategy $(\boldsymbol{\eta}^*, \zeta^*)$ for a portfolio of Term Insurance contracts, with payoff G^{TI} . Similarly to the case of Pure Endowment contracts, the optimal value process $V(\boldsymbol{\eta}^*, \zeta^*)$ is characterized by the relationship

$$\begin{aligned} V_t(\boldsymbol{\eta}^*, \zeta^*) &= \mathbb{E}^{\mathbb{Q}^*} [G^{TI} \mid \mathcal{G}_t] = \mathbb{E}^{\mathbb{Q}^*} \left[\int_0^T \sum_{i=1}^{\ell} \psi^i(u, X_u^{\pi^*})dH_u^i \mid \mathcal{G}_t \right] \\ &= \mathbb{E}^{\mathbb{Q}^*} \left[\int_0^T \sum_{i=1}^{\ell} (\psi^i(u, X_u^{\pi^*}) - \psi^i(u, X_{u-}^{\pi^*}))dH_u^i \mid \mathcal{G}_t \right] + \mathbb{E}^{\mathbb{Q}^*} \left[\int_0^T \sum_{i=1}^{\ell} \psi^i(u, X_{u-}^{\pi^*})dH_u^i \mid \mathcal{G}_t \right] \\ &= \int_0^t \sum_{i=1}^{\ell} \psi^i(u, X_{u-}^{\pi^*})dH_u^i + \mathbb{E}^{\mathbb{Q}^*} \left[\int_t^T \sum_{i=1}^{\ell} \psi^i(u, X_{u-}^{\pi^*})dH_u^i \mid \mathcal{G}_t \right], \quad t \in [0, T]. \end{aligned}$$

⁽⁶⁾The combination of Pure Endowment and Term Insurance unit linked is called Endowment Insurance and provides the payment of the benefit at the earliest of the time of death and maturity

Since the process $\{\psi^i(t, X_t^{\pi^*})\}_{t \in (0, T]}$ is \mathbb{G} -predictable, we obtain:

$$\begin{aligned}
V_t(\boldsymbol{\eta}^*, \zeta^*) &= \int_0^t \sum_{i=1}^{\ell} \psi^i(u, X_{u-}^{\pi^*}) dH_u^i + \mathbb{E}^{\mathbb{Q}^*} \left[\int_t^T \sum_{i=1}^{\ell} \psi^i(u, X_{u-}^{\pi^*}) (1 - H_u^i) \gamma_u^i du \mid \mathcal{G}_t \right] \\
&= \int_0^t \sum_{i=1}^{\ell} \psi^i(u, X_{u-}^{\pi^*}) dH_u^i + \int_t^T \sum_{i=1}^{\ell} \mathbb{E}^{\mathbb{Q}^*} \sum_{i=1}^{\ell} \left[\psi^i(u, X_{u-}^{\pi^*}) (1 - H_u^i) \gamma_u^i \mid \mathcal{G}_t \right] du \\
&= \int_0^t \sum_{i=1}^{\ell} \psi^i(u, X_{u-}^{\pi^*}) dH_u^i + \int_t^T \sum_{i=1}^{\ell} \mathbb{E}^{\mathbb{Q}^M} \left[\psi^i(u, X_{u-}^{\pi^*}) \mid \mathcal{F}_t \right] \mathbb{E}^{\mathbb{P}^I} \left[(1 - H_u^i) \gamma_u^i \mid \mathcal{H}_t \right] du \\
&= \int_0^t \sum_{i=1}^{\ell} \psi^i(u, X_{u-}^{\pi^*}) dH_u^i + \int_t^T U^i(u, t) B_t^i(u) du, \quad t \in [0, T],
\end{aligned}$$

where, for every $u \in [0, T]$, the processes $B^i(u) = \{B_t^i(u)\}_{t \in [0, u]}$ and $U^i(u, t) = \{U^i(u, t)\}_{t \in [0, u]}$ are respectively given by:

$$\begin{aligned}
B_t^i(u) &:= \mathbb{E}^{\mathbb{P}^I} \left[(1 - H_u^i) \gamma_u^i \mid \mathcal{H}_t \right], \\
U^i(u, t) &:= \mathbb{E}^{\mathbb{Q}^M} \left[\psi^i(u, X_u^{\pi^*}) \mid \mathcal{F}_t \right],
\end{aligned} \tag{6.9}$$

for all $t \in [0, u]$. We recall that $\psi^i(u, X_u^{\pi^*}) \in L^2(\mathcal{F}_u, \mathbb{P})$; then we assume that it admits the Föllmer–Schweizer decomposition with respect to $\tilde{\mathbf{S}}$ and \mathbb{F} , which is given by:

$$\psi^i(u, X_u^{\pi^*}) = U_0^i + \int_0^u \boldsymbol{\beta}_r^{i, \top}(u) d\tilde{\mathbf{S}}_r + A_u^i(u), \quad \bar{\mathbb{P}}\text{-a.s.}, \quad u \in [0, T],$$

where $U_0^i \in L^2(\mathcal{F}_0, \mathbb{P})$, $\boldsymbol{\beta}^i(u) := \{\boldsymbol{\beta}_t^i(u)\}_{t \in [0, u]} \in \Theta$, and $A^i(u) := \{A_t^i(u)\}_{t \in [0, u]}$ is a square-integrable (\mathbb{F}, \mathbb{P}) -martingale with $A_0^i(u) = 0$, strongly orthogonal to the martingale part of $\tilde{\mathbf{S}}$, for every $i = 1, \dots, \ell$. Since $\tilde{\mathbf{S}}$ is an $(\mathbb{F}, \mathbb{Q}^M)$ -martingale, we get that for every $0 \leq t \leq u \leq T$,

$$U^i(u, t) = \mathbb{E}^{\widehat{\mathbb{Q}}} \left[\psi^i(u, X_u^{\pi^*}) \mid \mathcal{F}_t \right] = U_0^i + \int_0^t \boldsymbol{\beta}_r^{i, \top}(u) d\tilde{\mathbf{S}}_r + A_t^i(u),$$

where $A^i(u)$ is a $(\mathbb{F}, \mathbb{Q}^M)$ -martingale by definition of the minimal martingale measure. Next, we assume some structure for the process $A^i(u)$. In particular, we assume that there exists a process $\varsigma^i(u) = \{\varsigma_t^i(u)\}_{t \in [0, u]}$ for every $u \in [0, T]$ such that

$$A_t^i(u) = \int_0^t \varsigma_r^i(u) dA_r^i, \quad t \in [0, u],$$

and that

$$\mathbb{E}^{\mathbb{P}} \left[\int_0^T \varsigma_t^{i, 2}(u) d\langle A^i \rangle_t \right] < \infty,$$

where A^i is a square-integrable $(\mathbb{F}, \mathbb{P}^M)$ -martingale, strongly orthogonal to the martingale part of $\tilde{\mathbf{S}}$. This assumption is rather general, and it follows from the martingale representation theorem for $(\mathbb{F}, \mathbb{P}^M)$ -martingales.

Proposition 6.10. *The insurance portfolio G^{TI} admits the Föllmer–Schweizer decomposition:*

$$G^{TI} = G_0^{TI} + \int_0^T \sum_{i=1}^{\ell} \left(\int_t^T B_{t-}^i(u) \boldsymbol{\beta}_t^{i, \top}(u) du \right) d\mathbf{S}_t + O_T \quad \mathbb{Q}^*\text{-a.s.},$$

where

$$\begin{aligned}
O_t &= \int_0^t \sum_{i=1}^{\ell} \psi^i(u, X_{u-}^{\pi^*}) (dH_u^i - (1 - H_u^i)\gamma_u^i) du \\
&\quad + \int_0^t \sum_{i=1}^{\ell} \left(\int_r^T U^i(u, r^-) \xi_r^i(u) du \right) (dH_r^i - (1 - H_r^i)\gamma_r^i) dr \\
&\quad + \int_0^t \sum_{i=1}^{\ell} \left(\int_r^T B_{r-}^i(u) \zeta_r^i(u) du \right) dA_r^i, \quad t \in [0, T],
\end{aligned}$$

$G_0^{TI} = \mathbb{E}^{\mathbb{Q}^*}[G^{TI} \mid \mathcal{H}_0]$, $B^i(u)$ is given by (6.9), $\beta^i(u)$ is the integrand in the Föllmer–Schweizer decomposition of $\psi^i(u, X_u^{\pi^*})$, and $\xi^i(u)$ is a suitable $(\mathcal{H}, \mathbb{P}^I)$ -predictable process in the martingale representation of $B^i(u)$. Then, the \mathbb{G} -pseudo-optimal strategy $(\boldsymbol{\eta}^*, \zeta^*)$ is given by:

$$\begin{aligned}
\boldsymbol{\eta}_t^* &= \int_t^T \sum_{i=1}^{\ell} B_{r-}^i(u) \beta_r^i(u) du, \quad t \in [0, T], \\
\zeta_t^* &= V_t(\boldsymbol{\eta}^*, \zeta^*) - \sum_{i=1}^{\ell} \left(\int_t^T B_{t-}^i(u) \beta_t^i(u) du \right)^\top \tilde{\mathbf{S}}_t, \quad t \in [0, T],
\end{aligned}$$

and the optimal value process $V(\boldsymbol{\eta}^*, \zeta^*)$ satisfies:

$$V_t(\boldsymbol{\eta}^*, \zeta^*) = G_0^{TI} + \int_0^t \boldsymbol{\eta}_r^{*\top} d\tilde{\mathbf{S}}_r + O_t, \quad t \in [0, T].$$

Proof. The proof replicates the lines of that of Proposition 6.8. □

7 Numerics

This section presents numerical results to validate the preceding theoretical findings. We introduce a Monte Carlo framework to evaluate and hedge unit-linked contract on the optimized green investment fund. The methodology involves two key steps: first, the implementation of efficient simulation schemes for the fund and its underlying carbon intensity process, and second, the use of conditioning techniques. This approach allows for variance reduction, enabling the efficient pricing and hedging of contracts such as Pure Endowments, Term Insurances, and Endowment Insurances.

7.1 An efficient scheme for the Fund

We assume that a given simulation scheme (exact or approximate) provides a discretized path for \mathbf{C} on a uniform time grid $\{jh \mid j = 0, \dots, N\}$, where the time step is $h = T/N$ for some $N \in \mathbb{N}^*$. We denote the discretized path of \mathbf{C} as $\widehat{\mathbf{C}} = (\widehat{C}_1, \dots, \widehat{C}_d)$.⁽⁷⁾ Let $\boldsymbol{\pi}^*$ be the optimal control map, and define the approximated optimal weights over the same uniform time grid as

$$\widehat{\boldsymbol{\pi}}_{kh} = \boldsymbol{\pi}^*(jh, \widehat{\mathbf{C}}_{jh}^N) \quad \text{for all } j \in \{0, \dots, N\}. \quad (7.1)$$

To introduce an efficient scheme for the fund $X^{\boldsymbol{\pi}^*}$, we use a conditioning technique which is well-known in the literature of schemes for stochastic volatility processes (see, e.g., the Heston exact scheme by Broadie and Kaya (2006), the SABR exact scheme by Cai et al. (2017), and the Heston second order

⁽⁷⁾The case of the CIR process is discussed at the end of this section.

scheme by Alfonsi and Lombardo (2025)). For hedging purposes, we consider the dynamics of the fund X^{π^*} under the minimal martingale measure \mathbb{Q}^M ,

$$dX_t^{\pi^*} = rX_t^{\pi^*} dt + X_t^{\pi^*} \pi_t^{*\top} \Sigma d\mathbf{Z}_t.$$

It is easy to see that, for every $t, s > 0$,

$$X_{t+s}^{\pi^*} = X_t^{\pi^*} \exp \left(\int_t^{t+s} \left(r - \frac{1}{2} \pi_u^{*\top} \Sigma \Sigma^\top \pi_u^* \right) du + \int_t^{t+s} \pi_u^{*\top} \Sigma d\mathbf{Z}_u \right),$$

Moreover, because of the independence between \mathbf{Z} and π^* , conditioning to the realization of $X_t^{\pi^*}$ and $\{\pi_u^*, u \in [t, t+s]\}$, the law of the ratio $X_{t+s}^{\pi^*}/X_t^{\pi^*}$ is

$$\log \mathcal{N} \left(\int_t^{t+s} \left(r - \frac{1}{2} \pi_u^{*\top} \Sigma \Sigma^\top \pi_u^* \right) du, \int_t^{t+s} \pi_u^{*\top} \Sigma \Sigma^\top \pi_u^* du \right),$$

where $\log \mathcal{N}(a, b)$ stands for lognormal distribution of mean a and variance b . The latter implies that we can simulate any marginal of the process X^{π^*} given a starting point, a discretization of the optimal weights process π^* as the one in (7.1) and a rule to discretize the integral depending on π^* (we use the trapezoidal rule). Therefore, an approximation of X^{π^*} over all the grid $\{jh \mid j = 0, \dots, N\}$, given $\hat{\pi}$, is

$$\begin{aligned} \hat{X}_0^N &= x, \\ \hat{X}_{(j+1)h}^N &= \hat{X}_{jh} \exp \left(rh - \frac{h}{4} (\hat{\pi}_{jh}^\top \Sigma \Sigma^\top \hat{\pi}_{jh} + \hat{\pi}_{(j+1)h}^\top \Sigma \Sigma^\top \hat{\pi}_{(j+1)h}) \right. \\ &\quad \left. + \sqrt{\frac{h}{2} (\hat{\pi}_{jh}^\top \Sigma \Sigma^\top \hat{\pi}_{jh} + \hat{\pi}_{(j+1)h}^\top \Sigma \Sigma^\top \hat{\pi}_{(j+1)h})} F_{j+1} \right), \quad \text{for all } j \in \{0, \dots, N-1\}, \end{aligned} \quad (7.2)$$

where $(F_j)_{j=0, \dots, N-1}$ is a set of i.i.d. standard Gaussian random variable independent of $\hat{\pi}$. For some products, as the Pure Endowment contracts, one needs only to simulate \hat{X} at maturity T ; in this case, one can save some computation time by using the following, equivalent in law, scheme

$$\begin{aligned} \hat{X}_T^N &= \hat{X}_0^N \exp \left(rT - \frac{h}{4} \sum_{j=0}^{N-1} (\hat{\pi}_{jh}^\top \Sigma \Sigma^\top \hat{\pi}_{jh} + \hat{\pi}_{(j+1)h}^\top \Sigma \Sigma^\top \hat{\pi}_{(j+1)h}) \right. \\ &\quad \left. + \sqrt{\frac{h}{2} \sum_{j=0}^{N-1} (\hat{\pi}_{jh}^\top \Sigma \Sigma^\top \hat{\pi}_{jh} + \hat{\pi}_{(j+1)h}^\top \Sigma \Sigma^\top \hat{\pi}_{(j+1)h})} F \right). \end{aligned} \quad (7.3)$$

where F is a standard Gaussian random variable independent of $\hat{\pi}$.⁽⁸⁾ A key advantage of these schemes is their efficiency. Indeed, rather than simulating the paths of all stocks, which would require d sets of Gaussian random variables, one can use a single set of Gaussian random variables, or, for specific cases as for example the Pure Endowment, even one random variable.

⁽⁸⁾We can follow the same steps for the dynamic under the physical measure \mathbb{P}^M . The construction is the same, and the extra drift term in the dynamic boils down to an extra factor $\exp \left(\frac{h}{2} \sum_{l=0}^j (\hat{\pi}_{lh} + \hat{\pi}_{(l+1)h})^\top (\boldsymbol{\mu} - \mathbf{1}r) \right)$ in the point $\hat{X}_{(j+1)h}^N$ for every $j \in \{0, \dots, N-1\}$.

A scheme for carbon intensity C: the example of the CIR process

In what follows, we present a numerical scheme for carbon intensity assuming that each component follows a Cox-Ingersoll-Ross (CIR) process, and we illustrate the efficient second-order scheme. For all $i \in \{1, \dots, d\}$ carbon intensity of each firm is

$$dC_{i,t} = \kappa_i (\bar{C}_i - C_{i,t}) dt + \lambda_i \sqrt{C_{i,t}} dW_{i,t}, \quad C_{i,0} = c_i.$$

Exact simulation schemes for the CIR process exist (e.g., based on CDF inversion or its representation as a Poisson weighted gamma mixture), but they are typically computationally intensive. This high cost makes them a suboptimal choice for our analysis, which relies on generating whole process trajectories. Therefore, we implement a multidimensional version of the well-known Ninomiya-Victoir scheme for the CIR process (see Alfonsi (2010) and Alfonsi and Lombardo (2024) for convergence, regularity results and extensions).⁽⁹⁾ We define the auxiliary maps

$$\eta_i(t, c, \omega) = \left(\kappa_i \bar{C}_i - \frac{\lambda_i^2}{4} \right) \psi_{\kappa_i} \left(\frac{t}{2} \right) + e^{-\kappa_i t/2} \kappa_i \left(\sqrt{\left(\kappa_i \bar{C}_i - \frac{\lambda_i^2}{4} \right) \psi_{\kappa_i} \left(\frac{t}{2} \right) + e^{-\kappa_i t/2} c + \frac{\lambda_i}{2} \omega} \right)^2,$$

where $\psi_{\kappa}(t) = (1 - e^{-\kappa t})/\kappa$ if $\kappa \neq 0$ and $\psi_{\kappa}(t) = t$ if $\kappa = 0$. Then, the second-order scheme $\hat{C} = (\hat{C}_1, \dots, \hat{C}_d)$ over the uniform grid $\{jh \mid j = 0, \dots, N\}$ is defined as follows

$$\begin{aligned} \hat{C}_{i,0}^N &= c_i, \\ \hat{C}_{i,(j+1)h}^N &= \eta_i(h, \hat{C}_{i,jh}^N, \sqrt{h}G_{i,j+1}), \quad \text{for all } j \in \{0, \dots, N-1\}, \end{aligned}$$

where $(G_{i,j})_{i=1, \dots, d, j=1, \dots, N}$ are i.i.d. standard Gaussian random variables.

7.2 Option evaluation and variance reduction formula

In this subsection, we provide estimators that allow fast pricing and hedging of the three contracts introduced earlier. These estimators are quite general but require an intensity model that allows fast computation (whether exact or approximate) of the quantities $\mathbb{P}^I(\tau > t)$ and $\mathbb{E}^{\mathbb{P}^I}[(1 - H_t)\gamma_t]$. Models with deterministic mortality intensity are a key example considered in Section 7.3.

Pure Endowment Contract

To explain this methodology we focus on one single Pure Endowment contract, with the benefit

$$\phi(X_T) = \min(K, \max(k, X_T)),$$

where $k \in [0, \infty)$ is the minimum guaranteed amount and $K \in [0, +\infty)$ is the maximum reimbursement. In this section we address the hedging problem for this specific structure of the payoff, although the procedure applies to more general cases. We will evaluate $\mathbb{E}_{0,x,c}^{\mathbb{Q}^*}[e^{-rT} \phi(X_T^{\pi^*}) \mathbb{1}_{\tau > T}]$ and its derivative $\partial_x \mathbb{E}_{0,x,c}^{\mathbb{Q}^*}[e^{-rT} \phi(X_T^{\pi^*}) \mathbb{1}_{\tau > T}]$.

A simple approach is to use the discretization scheme (7.3) of X^{π^*} and the independence of market and policyholder to get a candidate random variable to

$$\Upsilon_{PE}^{st}(N) = e^{-rT} \mathbb{P}^I(\tau > T) \phi(\hat{X}_{Nh}^N).^{(10)}$$

⁽⁹⁾Note that the scheme is well-defined if $\lambda_i^2 \leq 4\kappa_i \bar{C}_i$, which is weaker than the Feller's condition $\lambda_i^2 \leq 2\kappa_i \bar{C}_i$ for each i .

⁽¹⁰⁾The corresponding standard Monte Carlo estimator is the average of m samples.

We follow a different route. We leverage the conditional distribution of $\widehat{X} \mid \widehat{\pi}$ to define a new random variable with the same expected value but significantly reduced variance (see Table 7.2), thereby enhancing the efficiency of a Monte Carlo estimator. We state the following result.

Proposition 7.1. *Let $\Phi_{\mathcal{N}} : \mathbb{R} \rightarrow (0, 1)$ be the cumulative distribution function of a standard Gaussian random variable, for all $j \in \{1, \dots, N\}$ let*

$$v_{\widehat{\pi}}^j = \frac{h}{2} \sum_{l=0}^{j-1} (\widehat{\pi}_{lh}^{\top} \Sigma \Sigma^{\top} \widehat{\pi}_{lh} + \widehat{\pi}_{(l+1)h}^{\top} \Sigma \Sigma^{\top} \widehat{\pi}_{(l+1)h}),$$

and

$$a_{\widehat{\pi}}^j(y) = \frac{\log(y/x) - rT + \frac{1}{2}v_{\widehat{\pi}}^j}{\sqrt{v_{\widehat{\pi}}^j}}, \quad \text{and} \quad b_{\widehat{\pi}}^j(y) = a_{\widehat{\pi}}^j(y) - \sqrt{v_{\widehat{\pi}}^j}. \quad (7.4)$$

Then, given

$$\Upsilon_{PE}^{vr}(N) = e^{-rT} \left(k\Phi_{\mathcal{N}}(a_{\widehat{\pi}}^N(k)) + K\Phi_{\mathcal{N}}(-a_{\widehat{\pi}}^N(K)) + xe^{rT} (\Phi_{\mathcal{N}}(b_{\widehat{\pi}}^N(K)) - \Phi_{\mathcal{N}}(b_{\widehat{\pi}}^N(k))) \right) \mathbb{P}^I(\tau < T),$$

one has

$$\mathbb{E}_{0,x,\mathbf{c}}^{\mathbb{Q}^M}[\Upsilon_{PE}^{vr}(N)] = \mathbb{E}_{0,x,\mathbf{c}}^{\mathbb{Q}^M}[\Upsilon_{PE}^{st}(N)] \quad \text{and} \quad \text{Var}_{0,x,\mathbf{c}}^{\mathbb{Q}^M}[\Upsilon_{PE}^{vr}(N)] \leq \text{Var}_{0,x,\mathbf{c}}^{\mathbb{Q}^M}[\Upsilon_{PE}^{st}(N)].$$

We refer to Appendix D for the proof of this result.

Remark 7.2. 1) *Using the chain rule and simple algebra, we get a simple and elegant formula for the x -derivative of $\Upsilon_{PE}^{vr}(N)$. Indeed*

$$\partial_x \Upsilon_{PE}^{vr}(N) = e^{rT} (\Phi_{\mathcal{N}}(b_{\widehat{\pi}}^N(K)) - \Phi_{\mathcal{N}}(b_{\widehat{\pi}}^N(k))).$$

2) *We can quantify the difference of the variances in Proposition 7.1. Indeed, expanding the term $\text{Var}_{0,x,\mathbf{c}}^{\mathbb{Q}^M}(\Upsilon_{PE}^{st}(N) \mid v_{\widehat{\pi}}^N)$ and calculating $\mathbb{E}_{0,x,\mathbf{c}}^{\mathbb{Q}^M}[\Upsilon_{PE}^{st}(N)^2 \mid v_{\widehat{\pi}}^N]$ we get (in the sequel we drop the dependence on $0, x, \mathbf{c}$ in expectations and variances)*

$$\begin{aligned} & \text{Var}^{\mathbb{Q}^M}[\Upsilon_{PE}^{st}(N)] - \text{Var}^{\mathbb{Q}^M}[\Upsilon_{PE}^{vr}(N)] \\ &= e^{-2rt} \mathbb{E}^{\mathbb{Q}^M} \left[k^2 \Phi_{\mathcal{N}}(a_{\widehat{\pi}}^N(k)) + K^2 \Phi_{\mathcal{N}}(-a_{\widehat{\pi}}^N(K)) + x^2 e^{2rT} \exp\left(\sqrt{v_{\widehat{\pi}}^N}\right) (\Phi_{\mathcal{N}}(c_{\widehat{\pi}}^N(K)) - \Phi_{\mathcal{N}}(c_{\widehat{\pi}}^N(k))) \right. \\ & \quad \left. - \left(k\Phi_{\mathcal{N}}(a_{\widehat{\pi}}^N(k)) + K\Phi_{\mathcal{N}}(-a_{\widehat{\pi}}^N(K)) + xe^{rT} (\Phi_{\mathcal{N}}(b_{\widehat{\pi}}^N(K)) - \Phi_{\mathcal{N}}(b_{\widehat{\pi}}^N(k))) \right)^2 \right] \mathbb{P}^I(\tau < T)^2, \end{aligned}$$

$$\text{where } c_{\widehat{\pi}}^N(y) = a_{\widehat{\pi}}^N(y) - 2\sqrt{v_{\widehat{\pi}}^N}.$$

Term Insurance Contract

The Term Insurance contract is more intricate due to its path dependency. We consider a guaranteed minimum amount described by the function $k(t) \in [0, \infty)$ and a maximum possible payment function $K(t) \in [0, \infty]$, which in general depend on the date of death τ . Then the payoff is $\phi(t, x) = \min(K(t), \max(k(t), x))$ and want to evaluate $\mathbb{E}_{0,x,\mathbf{c}}^{\mathbb{Q}^*}[e^{-r\tau} \phi(\tau, X_{\tau}^{\pi^*}) \mathbf{1}_{\{\tau < T\}}]$ along with its derivative $\partial_x \mathbb{E}_{0,x,\mathbf{c}}^{\mathbb{Q}^*}[e^{-r\tau} \phi(\tau, X_{\tau}^{\pi^*}) \mathbf{1}_{\{\tau < T\}}]$ where $x = X_0^{\pi^*}$. Following the same procedure as for the Pure Endowment, we define the candidate random variable as

$$\Upsilon_{TI}^{st}(N) = \frac{1}{2} \sum_{j=0}^{N-1} (\phi(jh, \widehat{X}_{jh}^N) P_{jh} + \phi((j+1)h, \widehat{X}_{(j+1)h}^N) P_{(j+1)h}), \quad (7.5)$$

and we present a random variable with same expected value as (7.5), and a reduced variance (see Table 7.3). We state the following result, which is proved in appendix D.

Proposition 7.3. Let $\Phi_{\mathcal{N}} : \mathbb{R} \rightarrow (0, 1)$ be the cumulative distribution function of a standard Gaussian random variable, and $a_{\bar{\pi}}^j, b_{\bar{\pi}}^j$ defined in (7.4) for all $j \in \{1, \dots, N\}$. Define

$$\begin{aligned} \Upsilon_{TI}^{vr}(N) &= \frac{1}{2} \sum_{j=0}^{N-1} \left(k\Phi_{\mathcal{N}}(a_{\bar{\pi}}^j(k)) + K\Phi_{\mathcal{N}}(-a_{\bar{\pi}}^j(K)) + xe^{jh}(\Phi_{\mathcal{N}}(b_{\bar{\pi}}^j(K)) - \Phi_{\mathcal{N}}(b_{\bar{\pi}}^j(k))) \right) P_{jh} \\ &\quad + \left(k\Phi_{\mathcal{N}}(a_{\bar{\pi}}^{j+1}(k)) + K\Phi_{\mathcal{N}}(-a_{\bar{\pi}}^{j+1}(K)) + xe^{(j+1)h}(\Phi_{\mathcal{N}}(b_{\bar{\pi}}^{j+1}(K)) - \Phi_{\mathcal{N}}(b_{\bar{\pi}}^{j+1}(k))) \right) P_{(j+1)h} \end{aligned}$$

then

$$\mathbb{E}_{0,x,c}^{\mathbb{Q}^M}[\Upsilon_{TI}^{vr}(N)] = \mathbb{E}_{0,x,c}^{\mathbb{Q}^M}[\Upsilon_{TI}^{st}(N)] \quad \text{and} \quad \text{Var}_{0,x,c}^{\mathbb{Q}^M}[\Upsilon_{TI}^{vr}(N)] \leq \text{Var}_{0,x,c}^{\mathbb{Q}^M}[\Upsilon_{TI}^{st}(N)].$$

Endowment Insurance Contract

The Endowment Insurance contract is a mix of the two previous contracts. We consider a time dependent discounted payoff $\phi^{TI}(t, x) = \varrho e^{-rt} \min(K(t), \max(k(t), x))$, $\varrho \in (0, 1]$, that is paid upon policyholder's death at time $\tau \in [0, T)$ otherwise the benefit is paid at time T and is equal to $\phi^{PE}(x) = e^{-rT} \min(K(T), \max(k(T), x))$.

As usual, we need to approximate $\mathbb{E}_{0,x,c}^{\mathbb{Q}^*}[\phi^{PE}(\tau, X_{\tau}^{\pi^*})\mathbb{1}_{\{\tau < T\}} + \phi^{TI}(X_T^{\pi^*})\mathbb{1}_{\{\tau \geq T\}}]$ and its derivative $\partial_x \mathbb{E}_{0,x,c}^{\mathbb{Q}^*}[\phi^{PE}(\tau, X_{\tau}^{\pi^*})\mathbb{1}_{\{\tau < T\}} + \phi^{TI}(X_T^{\pi^*})\mathbb{1}_{\{\tau \geq T\}}]$ where $x = X_0^{\pi^*}$. Then one gets the following standard and variance-reduced random variables:

$$\Upsilon_{EI}^{st}(N) = \varrho \Upsilon_{TI}^{st}(N) + \Upsilon_{PE}^{st}(N), \quad \Upsilon_{EI}^{vr}(N) = \varrho \Upsilon_{TI}^{vr}(N) + \Upsilon_{PE}^{vr}(N).$$

Variance reduction Test

We present three Tables (7.2, 7.3 and 7.4) to measure the impact of the variance reduction formula. We consider a policyholder with a Gompertz-Makeham deterministic mortality intensity

$$\gamma_t = \xi + \frac{1}{b} \exp\left(\frac{\iota + t + m}{b}\right),$$

with the parameters

$$\xi = 0.0041959, \quad b = 11.5818911, \quad m = 79.6921211.$$

We fix the age of the policyholder $\iota = 60$. For the market, we consider four stocks with a set of parameters detailed in Table 7.1. In the following, we fix $K(t) = xe^{10rt}$ and $k(t) = xe^{rt}$ where r is the

	μ	σ					c	β	κ	λ		
S_1	0.25	0.30	$\rho =$	1.00	0.44	0.39	0.32	C_1	5000	2500	0.05	3.0
S_2	0.15	0.25		0.44	1.00	0.30	0.33	C_2	4000	2000	0.05	3.0
S_3	0.10	0.20		0.39	0.30	1.00	0.31	C_3	3000	1500	0.05	3.0
S_4	0.08	0.16		0.32	0.33	0.31	1.00	C_4	1000	500	0.05	3.0

(a) Parameters for the stock prices.

(b) Correlation matrix ρ .

(c) Parameters for the carbon intensities.

Table 7.1: Model parameters for the stocks, correlation matrix, and carbon intensities.

risk free rate and x is fund value at $t = 0$. We fix the following parameters,

$$\delta = 1, \quad \alpha = 0.0025, \quad r = 0.05, \quad x = 1.$$

We consider different maturities T taken from the set $\{5, 10, 20, 30\}$. Table 7.2 provides results for the Pure Endowment contract. We measure the Variance of $\Upsilon_{PE}^{st}(N)$ against the variance of $\Upsilon_{PE}^{vr}(N)$, obtaining an average of variance reduction of 99.9535%. This means that the statistical error obtained with M samples of $\Upsilon_{PE}^{st}(N)$ can be equivalently obtained by sampling only $\approx M/2150$ of $\Upsilon_{PE}^{vr}(N)$, which translates into a massive time gain.

	$T = 5$	$T = 10$	$T = 20$	$T = 30$
$\text{Var}(\Upsilon_{PE}^{st}(N))$	2.33245e-2	4.2705e-2	3.7802e-2	4.6313e-3
$\text{Var}(\Upsilon_{PE}^{vr}(N))$	7.3157e-6	2.0879e-5	2.1528e-5	2.2617e-6
Variance reduction	99.9686%	99.9511%	99.9431%	99.9511%

Table 7.2: Sample variance of $\Upsilon_{PE}(N)$. Number of samples: 10^6 . Discretization steps: $N = N(T) = 5T$.

For the Term Insurance (see Table 7.3), we still get very good results with an average variance reduction of 97.4639%. This means that using $\Upsilon_{PE}^{vr}(N)$ requires approximately 1/40th the number of samples, compared to the standard $\Upsilon_{PE}^{st}(N)$. Finally, Table 7.4 summarizes the results for the

	$T = 5$	$T = 10$	$T = 20$	$T = 30$
$\text{Var}(\Upsilon_{TI}^{st}(N))$	6.4640e-6	4.5424e-5	4.2306e-4	1.1124e-3
$\text{Var}(\Upsilon_{TI}^{vr}(N))$	2.5549e-8	5.7513e-7	1.3889e-5	5.7844e-5
Variance reduction	99.6047%	98.7339%	96.7170%	94.7999%

Table 7.3: Sample variance of $\Upsilon_{TI}(N)$. Number of samples: 10^6 . Discretizations step: $N = N(T) = 5T$.

Endowment insurance, which are similar to the Pure Endowment for maturities $T = 5, 10, 20$ and to the Term Insurance for $T = 30$. This is consistent with the contract structure that behaves as the Pure Endowment for short maturities and more like the Term Insurance for longer maturities.

	$T = 5$	$T = 10$	$T = 20$	$T = 30$
$\text{Var}(\Upsilon_{EI}^{st}(N))$	2.3378e-2	4.2908e-2	3.9107e-2	5.9768e-3
$\text{Var}(\Upsilon_{EI}^{vr}(N))$	8.1701e-6	2.8083e-5	6.8198e-5	8.1028e-5
Variance reduction	99.9651%	99.93454%	99.8256%	98.6443%

Table 7.4: Sample variance of $\Upsilon_{EI}(N)$. Number of samples: 10^6 . Discretizations step: $N = N(T) = 5T$.

Overall, the results of variance reduction are very satisfying. Indeed, in the worst case (Term Insurance contract with $T = 30$), we still get a variance-reduction of 94.7999%, which means that we need to simulate only $\approx 5\%$ of the samples with respect to the standard case.

7.3 Hedging results

The insurance payoffs that we aim to hedge are subject to three sources of risk, namely market risk, carbon risk and mortality risk. The primary risk that can be hedged via risk minimization using traditional financial instruments is market risk. It is clear from the computations of the error-minimizing strategy that both carbon and mortality risk cannot be perfectly hedged, due to the lack of financial instruments that can be used for the scope, hence they enter in the strategy costs. From a mathematical perspective these two sources of risk contribute the orthogonal martingale. While unhedgeable in the conventional sense, carbon and mortality risk can be efficiently reduced

through structural and strategic design choices. Specifically, carbon risk is mitigated ex-ante through the construction of the ad-hoc investment fund, by selecting assets that exhibit low carbon intensity. Mortality risk, on the other hand, can be diversified when considering large portfolios of insurance policies, in view of the law of large numbers. In that regard, Figure 7.1 illustrates the distribution of the hedging cost of continuously rebalanced hedging strategies for three types of unit-linked contracts (Pure Endowment, Term Insurance, and Endowment Insurance) with a maturity $T = 20$ years and the initial fund value $x = 1$. Each panel corresponds to a different contract type and displays the distribution for a single policy and the distribution for a portfolio of 1000 policies. In both cases, costs are small on average (for the Pure endowment contract, single policyholder, the average loss is -0.0171 and for the case of 1000 policyholders is -0.00160). However, these plots confirm that the hedging is more efficient when considering large portfolios of insurance policies, for which we observe considerably less dispersion. For example, the standard deviation of the pure endowment and single policy holder is 3.8281, whereas for the case of 1000 contracts is 0.1184. All the results of the current section are obtained on 10000 simulations. Figure 7.2 shows the distribution of the hedging cost for

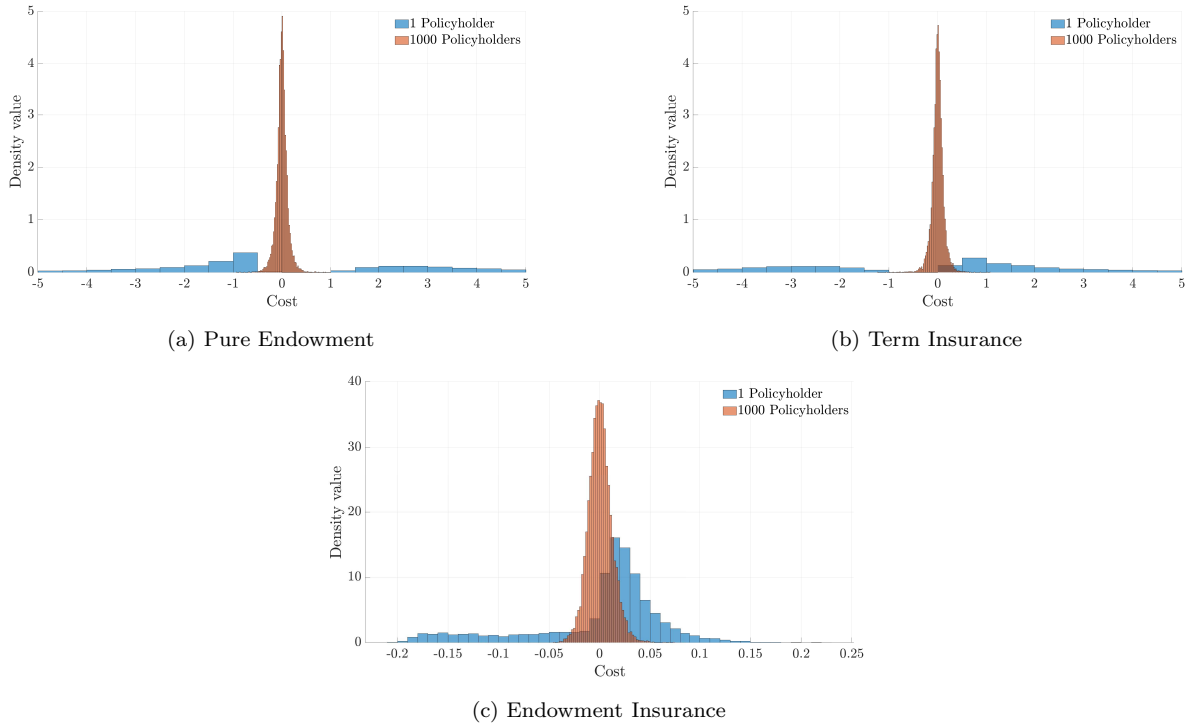


Figure 7.1: Cost of the continuous hedging: 1 Policyholder Vs Portfolio of 1000 Policyholders.

a homogeneous portfolio of 1000 life insurance contract, with policy holder's initial age of 60 years. We analyse Pure Endowment on the upper left panel, Term Insurance on the upper right panel, and Endowment Insurance on the lower panel. Our goal is to compare three different strategies: the continuous hedging strategy via risk minimization, the static strategy, and no-hedging. Specifically, we refer to the static hedging case when the replicating portfolio is constructed at time $t = 0$, and the optimal portfolio weights are not updated until maturity. No hedging corresponds to the case where the insurer collects the policy premiums at time $t = 0$ and deposits the entire amount in the bank account, using it to pay the policyholder benefits at maturity. We observe that no hedging is by far the most costly approach, with an average loss of 5.842 and standard deviation of 2.84 for the Pure endowment case (note that the plot of the density function is truncated, and for example the

90% quantile is $q_{90} = 9.362$). The static hedging shows both profits and losses, although on average we observe losses of 2.194. This implies that static hedging is an improvement over the unhedged payoffs, but variability is still quite high, equal to 1.807. The dynamic risk minimizing strategy on the other hand significantly reduces both the average loss, which is equal to -0.0016 , and the variability, with a standard deviation 0.1184. The behaviour of the strategies for the case of Term insurance and Endowment insurance is similar and the numbers are reported in Table 7.5.

Pure Endowment			
	No Hedging	Static Hedging	Continuous Hedging
Mean	5.842	2.186	-0.0016
St. Dev.	2.84	1.807	0.1184
Term Insurance			
	No Hedging	Static Hedging	Continuous Hedging
Mean	1.863	0.503	-0.0004
St. Dev.	0.184	0.474	0.121
Endowment Insurance			
	No Hedging	Static Hedging	Continuous Hedging
Mean	7.721	2.708	0.0006
St. Dev.	2.846	1.727	0.012

Table 7.5: Mean and standard deviation of the distribution of the hedging cost for a portfolio of 1000 pure endowment policies (top panel), term insurance policies (middle panel), and endowment insurance policies (bottom panel) under no hedging, static hedging, and continuous hedging.

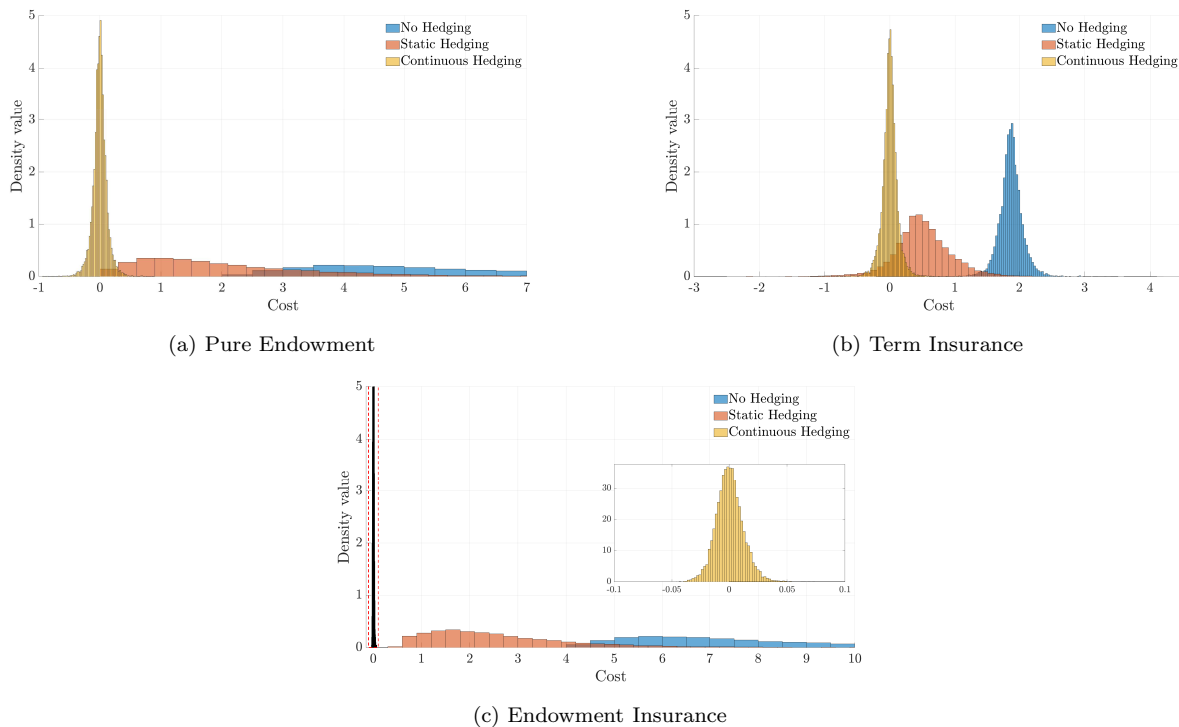


Figure 7.2: Cost of different hedging strategies

We remark that the analyses presented in Figures 7.1 and 7.2 are conducted on policies written on

homogeneous policyholders, all aged $\iota = 60$ at time $t = 0$. In contrast, Figure 7.3 shows the distribution of the hedging cost for a portfolio of policies written on heterogeneous policyholders, whose initial ages range from 55 to 65 years. This picture shows similar outcomes for the two portfolios, revealing that the approach is robust across ages.

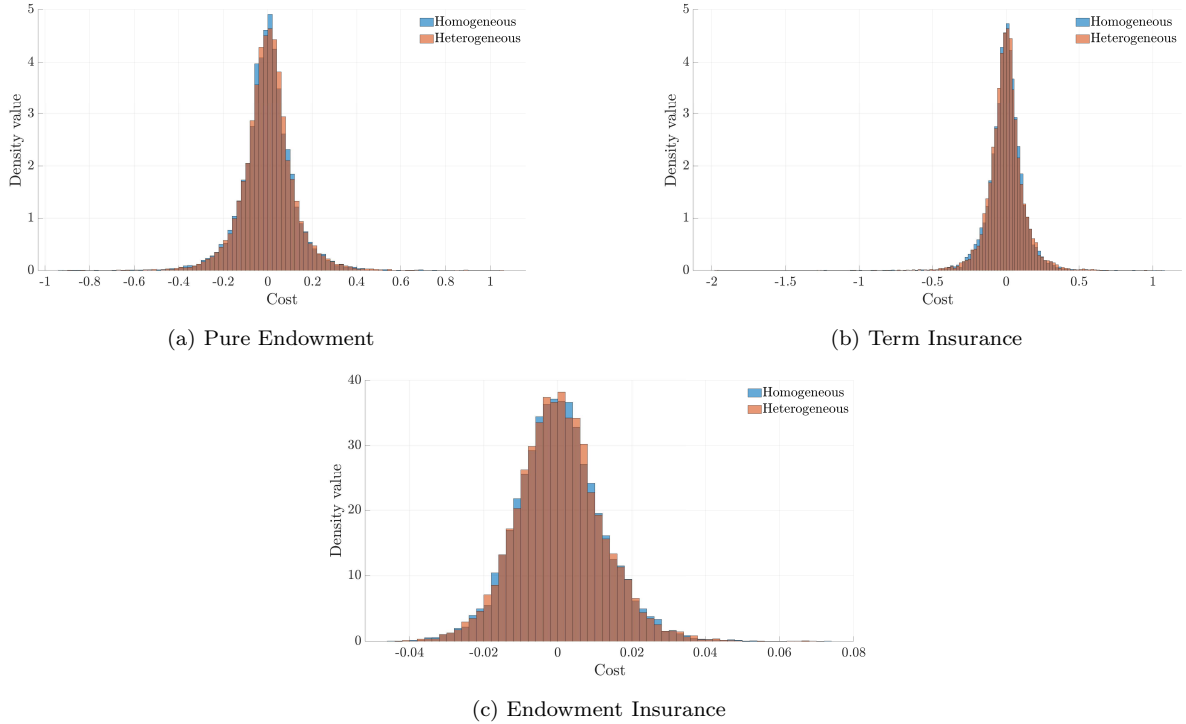


Figure 7.3: Cost of the continuous hedging: 1 Homogeneous group Vs 10 Heterogeneous groups.

8 Concluding remarks

In this paper, we develop a comprehensive framework for designing a carbon-efficient investment fund and the hedging of unit-linked life insurance policies linked to that investment fund. Hence, these insurance products are subject to market, carbon, and mortality risks. On the asset management side, we introduce a novel portfolio selection methodology that integrates carbon aversion directly into the fund manager’s preferences by embedding a penalty term in the objective function. The novelty of this approach is that it does not reduce to a naive exclusion of high-carbon-intensity stocks; instead, it implements a realistic and flexible trade-off between each stock’s risk–return profile and its associated carbon footprint. We solve the optimization problem using classical dynamic programming techniques under several alternative specifications for the dynamics of the carbon-intensity process, including Ornstein-Uhlenbeck, CIR and continuous finite-state Markov chain. From the theoretical point of view, we prove a Verification theorem and for each of these cases we give conditions for the existence of the solution of the value function. Empirical results on S&P500 data confirm that even moderate levels of carbon aversion can significantly reduce portfolio carbon intensity.

On the insurance side, we hedge three unit-linked policies having the optimized carbon-penalized investment fund as underlying. We used quadratic hedging to minimize the L^2 tracking error and test numerically the performance of the error-minimising strategy. The results highlight that this dynamic hedging strategy outperforms the other hedging approaches by a large margin. An important aspect,

from a numerical perspective, is that we combine a potential weak second-order simulation scheme for the optimized investment fund dynamics with conditioning-based variance reduction to compute the risk-minimizing strategy accurately and at low computational cost. Overall, the paper bridges optimal investment fund design and hedging strategy in a single setting, providing theory and implementable numerics for the development and risk management of sustainable unit-linked products.

Our study offers several possibilities for extensions. For example, following Ceci et al. (2022), the framework could be enriched by introducing dependence between the financial market and the insurance framework, e.g., through some common risk factors. This would allow for the analysis of systemic shocks, such as pandemics or natural catastrophes, and their joint impact on financial performance and mortality risk. This setup would bring to a more involved optimization problem and therefore is left to future research.

Appendix

A Proofs of some technical results of Section 3

A.1 Proof of Theorem 3.5

Consider the function $w(t, x, \mathbf{c})$. Since this function is regular we apply Itô formula

$$\begin{aligned} w(T, \tilde{X}_T^\pi, \mathbf{C}_T) &= w(t, x, \mathbf{c}) + \int_t^T \left\{ \partial_t w(s, \tilde{X}_s^\pi, \mathbf{C}_s) + \mathcal{L}w(s, \tilde{X}_s^\pi, \mathbf{C}_s) \right\} ds \\ &\quad + \int_t^T \partial_x w(s, \tilde{X}_s^\pi, \mathbf{C}_s) \tilde{X}_s^\pi \boldsymbol{\pi}_s^\top \boldsymbol{\Sigma} d\mathbf{Z}_s + \sum_{i=1}^d \int_t^T \partial_{c_i} w(s, \tilde{X}_s^\pi, \mathbf{C}_s) dM_s^{i, cont} \\ &\quad + \int_t^T \int_{\mathcal{Z}} \Delta_z w(s, \tilde{X}_s^\pi, \mathbf{C}_s) (m(ds, dz) - \nu_s(dz) ds), \end{aligned}$$

with $\Delta_z w(s, \tilde{X}_s^\pi, \mathbf{C}_s) = w(s, \tilde{X}_s^\pi, \mathbf{C}_{s-} + z) - w(s, \tilde{X}_s^\pi, \mathbf{C}_{s-})$, and where we intend X_s^π, \mathbf{C}_s as the processes at time s , starting at time t at values x, \mathbf{c} . We define the increasing sequence of stopping times as follows. We fix $t \geq 0$ and let, for every $u > t$

$$\begin{aligned} I_u^1 &:= \int_t^u (\partial_x w(s, \tilde{X}_s^\pi, \mathbf{C}_s) \tilde{X}_s^\pi)^2 \boldsymbol{\pi}_s^\top \boldsymbol{\Sigma} \boldsymbol{\Sigma}^\top \boldsymbol{\pi}_s ds, \\ I_u^2 &:= \sum_{i=1}^d \int_t^u \left(\partial_{c_i} w(s, \tilde{X}_s^\pi, \mathbf{C}_s) \right)^2 d\langle M^{i, cont} \rangle_s, \\ I_u^3 &:= \int_t^u \left(\sup_{\mathcal{Z}} \Delta_z w(s, \tilde{X}_s^\pi, \mathbf{C}_s) \right)^2 \nu_s(\mathcal{Z}) ds; \end{aligned}$$

then we define

$$\tau_n = \inf \{ u \geq t : I_u^1 + I_u^2 + I_u^3 \geq n \}.$$

Then, we get that

$$\begin{aligned} w(T \wedge \tau_n, \tilde{X}_{T \wedge \tau_n}^\pi, \mathbf{C}_{T \wedge \tau_n}) &= w(t, x, \mathbf{c}) + \int_t^{T \wedge \tau_n} \left\{ \partial_t w(s, \tilde{X}_s^\pi, \mathbf{C}_s) + \mathcal{L}w(s, \tilde{X}_s^\pi, \mathbf{C}_s) \right\} ds \\ &\quad + \int_t^{T \wedge \tau_n} \partial_x w(s, \tilde{X}_s^\pi, \mathbf{C}_s) \tilde{X}_s^\pi \boldsymbol{\pi}_s^\top \boldsymbol{\Sigma} d\mathbf{Z}_s + \sum_{i=1}^d \int_t^{T \wedge \tau_n} \partial_{c_i} w(s, \tilde{X}_s^\pi, \mathbf{C}_s) dM_s^{i, cont} \\ &\quad + \int_t^{T \wedge \tau_n} \int_{\mathcal{Z}} \Delta_z w(s, \tilde{X}_s^\pi, \mathbf{C}_s) (m(ds, dz) - \nu_s(dz) ds). \end{aligned}$$

Since w satisfies the equation (3.5), we get that

$$\begin{aligned} w(T \wedge \tau_n, \tilde{X}_{T \wedge \tau_n}^\pi, \mathbf{C}_{T \wedge \tau_n}) &\leq w(t, x, \mathbf{c}) \\ &+ \int_t^{T \wedge \tau_n} \partial_x w(s, \tilde{X}_s^\pi, \mathbf{C}_s) \tilde{X}_s^\pi \pi_s^\top \Sigma d\mathbf{Z}_s + \sum_{i=1}^d \int_t^{T \wedge \tau_n} \partial_{c_i} w(s, \tilde{X}_s^\pi, \mathbf{C}_s) dM_s^{i, cont} \\ &+ \int_t^{T \wedge \tau_n} \int_{\mathcal{Z}} \Delta_z w(s, \tilde{X}_s^\pi, \mathbf{C}_s) (m(ds, dz) - \nu_s(dz) ds). \end{aligned}$$

Taking the expectation on both sides of the inequality, using that π is an admissible control and that w satisfies the growth condition, and the terminal condition of the Hamilton Jacobi Bellman equation, we get that

$$w(t, x, \mathbf{c}) \geq \mathbb{E}^{\mathbb{P}^M} [w(T \wedge \tau_n, \tilde{X}_{T \wedge \tau_n}^\pi, \mathbf{C}_{T \wedge \tau_n})].$$

Next, we take the limit at $n \rightarrow \infty$, and using Lebesgue dominated convergence theorem we get that

$$w(t, x, \mathbf{c}) \geq \mathbb{E}^{\mathbb{P}^M} [U(\tilde{X}_T^\pi)],$$

hence $w(t, x, \mathbf{c}) \geq v(t, x, \mathbf{c})$. This shows point *i.* of the statement. Moreover, the equality holds for the maximiser π^* , which concludes the proof.

A.2 Proof of Theorem 3.6

Suppose that a classical solution w of the Hamilton Jacobi Bellman equation (3.5) can be written as

$$w(t, x, \mathbf{c}) = \begin{cases} \frac{x^{1-\delta}}{1-\delta} \varphi(t, \mathbf{c}), & \delta \in (0, 1) \cup (1, +\infty), \\ \log(x) + \varphi(t, \mathbf{c}), & \delta = 1, \end{cases}$$

where φ does not depend on x and it is a positive function. We let $\Phi^\pi(t, \mathbf{c})$ be defined as

$$\Phi^\pi(t, \mathbf{c}) := \pi^\top (\boldsymbol{\mu} - \mathbf{1}r) - \frac{1}{2} \pi^\top \left(\delta \Sigma \Sigma^\top + \mathbf{e}(t, \mathbf{c}) \odot \mathbf{D}\mathbf{D}^\top \right) \pi.$$

Then, we can rewrite the equation (3.5) as follows.

(i) If $\delta \in (0, 1) \cup (1, +\infty)$, we get that (3.5) is equivalent to

$$\begin{cases} \partial_t \varphi(t, \mathbf{c}) + \mathcal{L}^{\mathbf{C}} \varphi(t, \mathbf{c}) + \varphi(t, \mathbf{c}) \left[(1-\delta)r + (1-\delta) \max_{\pi \in [-\Xi, \Xi]^d} \Phi^\pi(t, \mathbf{c}) \right] = 0, & (t, \mathbf{c}) \in [0, T] \times \mathcal{D}, \\ \varphi(t, \mathbf{c}) = 1, & \mathbf{c} \in \mathcal{D}. \end{cases} \quad (\text{A1})$$

(ii) If $\delta = 1$, corresponding the logarithmic case, the equation (3.5) becomes:

$$\begin{cases} \partial_t \varphi(t, \mathbf{c}) + r + \mathcal{L}^{\mathbf{C}} \varphi(t, \mathbf{c}) + \max_{\pi \in [-\Xi, \Xi]^d} \Phi^\pi(t, \mathbf{c}) = 0, & (t, \mathbf{c}) \in [0, T] \times \mathcal{D}, \\ \varphi(T, \mathbf{c}) = 0, & \mathbf{c} \in \mathcal{D}. \end{cases} \quad (\text{A2})$$

We let $\pi^* := \arg \max \Phi^\pi(t, \mathbf{c})$. Taking the gradient and the Hessian of Φ^π with respect to π we get that

$$\begin{aligned} \nabla_\pi \Phi^\pi(t, \mathbf{c}) &= (\boldsymbol{\mu} - \mathbf{1}r) - \left(\delta \Sigma \Sigma^\top + \mathbf{e}(t, \mathbf{c}) \odot \mathbf{D}\mathbf{D}^\top \right) \pi, \\ \text{Hess}_\pi \Phi^\pi(t, \mathbf{c}) &= -(\delta \Sigma \Sigma^\top + \mathbf{e}(t, \mathbf{c}) \odot \mathbf{D}\mathbf{D}^\top). \end{aligned}$$

Then, setting $\nabla_{\boldsymbol{\pi}} \Phi^{\boldsymbol{\pi}}(t, \mathbf{c}) = \mathbf{0}$, provides the candidate optimal strategy $\boldsymbol{\pi}^*(t, \mathbf{c})$ given by (3.7). Moreover, since $\text{Hess}_{\boldsymbol{\pi}} \Phi^{\boldsymbol{\pi}}(t, \mathbf{c})$ is negative definite for every $\boldsymbol{\pi}$, this ensure that $\boldsymbol{\pi}^*(t, \mathbf{c})$ in equation (3.7) is the well defined global maximizer. Next we show that $\boldsymbol{\pi}^*(t, \mathbf{c})$ is an admissible control. We note that

$$\begin{aligned} \|\boldsymbol{\pi}^*(t, \mathbf{c})\| &\leq \max \left(\text{Sp} \left(\left(\delta \boldsymbol{\Sigma} \boldsymbol{\Sigma}^{\top} + \mathbf{e}(t, \mathbf{c}) \odot \mathbf{D} \mathbf{D}^{\top} \right)^{-1} \right) \right) \|\boldsymbol{\mu} - \mathbf{1}r\| \\ &\leq \frac{\|\boldsymbol{\mu} - \mathbf{1}r\|}{\min(\text{Sp}(\delta \boldsymbol{\Sigma} \boldsymbol{\Sigma}^{\top} + \mathbf{e}(t, \mathbf{c}) \odot \mathbf{D} \mathbf{D}^{\top}))} \\ &\leq \frac{\|\boldsymbol{\mu} - \mathbf{1}r\|}{\min(\text{Sp}(\delta \boldsymbol{\Sigma} \boldsymbol{\Sigma}^{\top}))}, \end{aligned}$$

where $\text{Sp}(\cdot)$ denotes the spectrum of a matrix. Hence, for every $\Xi > \frac{\|\boldsymbol{\mu} - \mathbf{1}r\|}{\min(\text{Sp}(\delta \boldsymbol{\Sigma} \boldsymbol{\Sigma}^{\top}))}$ we get that $\boldsymbol{\pi}^*(t, \mathbf{c}) \in (-\Xi, \Xi)^d$ for every $(t, \mathbf{c}) \in [0, T] \times \mathcal{D}$. Replacing $\boldsymbol{\pi}$ with $\boldsymbol{\pi}^*$ in equations (A1) and (A2) yields the Cauchy problem in equation (3.6). If φ is a classical solution of (3.6), then w is also regular and $|w(t, x, \mathbf{c})| \leq K(1 + |x| + |x|^{1-\delta})$ and solves (3.5), hence the result follows from Theorem 3.5.

B Proofs of some technical results of Section 4

B.1 Proof of Corollary 4.2

Let $S \in [0, T]$, $\mathcal{R} = (\frac{1}{R}, R)^d$, for some $R > 1$, $Q = [0, S] \times \mathcal{R}$ and consider the PDE with final condition

$$\begin{cases} \partial_t v(t, \mathbf{c}) + \mathcal{L}^{\mathbf{C}} v(t, \mathbf{c}) + H(\mathbf{c})v(t, \mathbf{c}) = f(t, \mathbf{c}), & \text{in } Q, \\ v(t, \mathbf{c}) = \varphi(t, \mathbf{c}), & \text{in } \partial_0 Q, \end{cases} \quad (\text{B1})$$

$\partial_0 Q$ denoting the parabolic boundary of Q . Under the assumption that $\alpha_i(t)$ are Lipschitz continuous for every $i = 1, \dots, d$, it holds that H and f are Lipschitz continuous and bounded; then, they are in particular p -Hölder continuous for all $p \in (0, 1)$, so the coefficients of the PDE (B1) satisfy in Q all the assumptions of, e.g. Theorem 9 and Corollary 2 in Chapter 3, Sec. 4 in Friedman (2008). Therefore a unique bounded solution $v \in C^{1,2}([0, S] \times \mathcal{R}) \cap C([0, S] \times \bar{\mathcal{R}})$, with $\bar{\mathcal{R}} = [\frac{1}{R}, R]^d$, exists. We let $\tau_{\mathcal{R}}$ be the first exit time of the process \mathbf{C} starting in $(t, \mathbf{c}) \in [0, S] \times \mathcal{R}$ from the set \mathcal{R} , i.e.

$$\tau_{\mathcal{R}} = \inf\{s > t : \mathbf{C}_s \notin \mathcal{R}\}.$$

We define, for every $t < s$

$$Z_s := \exp \left(\int_t^{s \wedge \tau_{\mathcal{R}}} H(u, \mathbf{C}_u) du \right) v(s, \mathbf{C}_s) - \int_t^{s \wedge \tau_{\mathcal{R}}} \exp \left(\int_t^u H(r, \mathbf{C}_r) dr \right) f(u, \mathbf{C}_u) du,$$

then $(Z_s)_{s \in [t, T \wedge \tau_{\mathcal{R}}]}$ is a martingale. Moreover, it holds that $(S \wedge \tau_{\mathcal{R}}, \mathbf{C}_{S \wedge \tau_{\mathcal{R}}}) \in \partial_0 Q$, then,

$$\begin{aligned} v(t, \mathbf{c}) &= \mathbb{E}^{t, \mathbf{c}}(Z_t) = \mathbb{E}^{t, \mathbf{c}}(Z_{S \wedge \tau_{\mathcal{R}}}) \\ &= \mathbb{E}^{t, \mathbf{c}} \left[\exp \left(\int_t^{S \wedge \tau_{\mathcal{R}}} H(s, \mathbf{C}_s) ds \right) \varphi(S \wedge \tau_{\mathcal{R}}, \mathbf{C}_{S \wedge \tau_{\mathcal{R}}}) - \int_t^{S \wedge \tau_{\mathcal{R}}} \exp \left(\int_t^s H(u, \mathbf{C}_u) du \right) f(s, \mathbf{C}_s) ds \right]. \end{aligned}$$

By the strong Markov property,

$$\begin{aligned} &\varphi(S \wedge \tau_{\mathcal{R}}, \mathbf{C}_{S \wedge \tau_{\mathcal{R}}}) \\ &= \mathbb{E} \left[\exp \left(\int_{S \wedge \tau_{\mathcal{R}}}^T H(s, \mathbf{C}_s) ds \right) \mathbf{1}_{\{\delta \in (0, 1) \cup (1, +\infty)\}} - \int_{S \wedge \tau_{\mathcal{R}}}^T \exp \left(\int_t^s H(u, \mathbf{C}_u) du \right) f(s, \mathbf{C}_s) ds \mid \mathcal{F}_{S \wedge \tau_{\mathcal{R}}} \right]. \end{aligned}$$

By replacing above, it follows that $v \equiv \varphi$ in Q , for each S and R . Hence, we get that $\varphi(t, \mathbf{c})$ is a solution of (3.6).

Next we show uniqueness. Assume that the Feller condition holds, i.e. $2\lambda_i \bar{C}_i \geq \lambda_i^2$ for all i . Let $v \in \mathcal{C}([0, T] \times (0, \infty)^n)$ denote a solution to (3.6). We prove that $v = \varphi$. Let $S_n < T$ and let $\mathcal{R}_n = (\frac{1}{R_n}, R_n)^d$ denote a sequence of rectangles, such that $Q_n = [0, S_n) \times \mathcal{R}_n \uparrow [0, T) \times (0, \infty)^n$. Let v_n be the unique solution to

$$\begin{cases} \partial_t v_n(t, \mathbf{c}) + \mathcal{L}^{\mathbf{C}} v_n(t, \mathbf{c}) + H(t, \mathbf{c}) v_n(t, \mathbf{c}) = f(t, \mathbf{c}), & \text{in } Q_n, \\ v_n(t, \mathbf{c}) = v(t, \mathbf{c}), & \text{in } \partial_0 Q_n. \end{cases} \quad (\text{B2})$$

Since v trivially solves the above PDE problem (B2), by uniqueness, we get that $v_n = v$ and

$$v(t, \mathbf{c}) = \mathbb{E}^{t, x, y} \left[\exp \left(\int_t^{S_n \wedge \tau_{\mathcal{R}_n}} H(s, \mathbf{C}_s) ds \right) v(S_n \wedge \tau_{\mathcal{R}_n}, \mathbf{C}_{S_n \wedge \tau_{\mathcal{R}_n}}) - \int_t^{S_n \wedge \tau_{\mathcal{R}_n}} \exp \left(\int_t^s H(u, \mathbf{C}_u) du \right) f(s, \mathbf{C}_s) ds \right].$$

By Feller condition we get that, for a process \mathbf{C} starting at t at value $\mathbf{C}_t = \mathbf{c}$, with $c_i > 0$ for every $i = 1, \dots, d$, $\mathbb{P}(\mathbf{C}_s \in (0, \infty)^d, \text{ for all } s) = 1$. Then, taking $n \rightarrow \infty$, one has $\tau_{\mathcal{R}_n} \uparrow \infty$ and since v is continuous, we obtain $v \equiv \varphi$.

C Proofs of some technical results of Section 6

C.1 Proof of Proposition 6.8

Using equations (6.4), (6.6), and (6.5), and applying Itô product rule, we compute:

$$d\mathbb{E}^{\mathbb{Q}^*} [G^{PE} | \mathcal{G}_t] = \sum_{i=1}^{\ell} B_{t-}^i dU_t^i + U_{t-}^i dB_t^i, \quad (\text{C1})$$

where the equality follows from independence of the financial market and the insured individuals, hence $\langle B^i, U^i \rangle_t = 0$ and $\sum_{s \leq t} \Delta B_s^i \Delta U_s^i = 0$. Therefore we get that equation (C1) becomes

$$\sum_{i=1}^{\ell} B_{t-}^i \beta_t^{i, \top} d\mathbf{S}_t + \sum_{i=1}^{\ell} B_{t-}^i dA_t^i + \sum_{i=1}^{\ell} U_{t-}^i \xi_t^i (dH_t^i - (1 - H_t^i) \gamma_t^i dt).$$

Note that $\{\sum_{i=1}^{\ell} B_{t-}^i \beta_t^i\}_{t \in [0, T]}$ belongs to $\Theta(\mathbb{G})$. Moreover the process O satisfies

$$dO_t = \sum_{i=1}^{\ell} B_{t-}^i dA_t^i + \sum_{i=1}^{\ell} U_{t-}^i \xi_t^i (dH_t^i - (1 - H_t^i) \gamma_t^i dt)$$

and it is a square-integrable $(\mathbb{G}, \mathbb{Q}^*)$ -martingale. This concludes the proof.

C.2 Proof of Proposition 6.9

First, we observe that the PDE (6.8) has a unique classical solution under very general conditions on the infinitesimal generator $\mathcal{L}^{\mathbf{C}}$, see, e.g. Colaneri and Frey (2021). From (Ceci et al., 2015, Proposition 6.2) we get that $V_t(\tilde{\varphi}^i)$ is given by

$$V_t(\tilde{\varphi}^i) = U_0^i + \int_0^t \beta_u^i \frac{dX_t^{\pi^*}}{X_t^{\pi^*}} + A_t^i,$$

where

$$\beta_t^i = (X_t^{\pi^*})^2 \frac{d(V_t(\tilde{\varphi}^i), X_t^{\pi^*})_t}{\frac{d(X_t^{\pi^*})_t}{dt}}.$$

Next, we observe that, using Markovianity

$$V_t(\tilde{\varphi}^i) = \mathbb{E}^{\mathbb{Q}^M} \left[\phi^i(X_T^{\pi^*}) | \mathcal{F}_t \right] = F^i(t, X_t^{\pi^*}, \mathbf{C}_t).$$

Moreover, $V_t(\tilde{\varphi}^i)$ is a $(\mathbb{F}, \mathbb{Q}^M)$ martingale, which implies that the function $F(t, x, \mathbf{c})$ is the solution of (6.8). Hence $\beta_t^i = \frac{\partial F^i}{\partial x}(t, X_t^{\pi^*}, \mathbf{C}_t)$. To conclude we note that $\frac{dX_t^{\pi^*}}{X_t^{\pi^*}} = \boldsymbol{\pi}_u^{*\top} d\tilde{\mathbf{S}}_t$.

D Proofs of some technical results of Section 7

D.1 Proof of Proposition 7.1

From the definition of $v_{\hat{\pi}}^N$ and (7.3), we get that $\hat{X}_T^N = x \exp(rT - \frac{1}{2}v_{\hat{\pi}}^N + \sqrt{v_{\hat{\pi}}^N}F)$

$$\begin{aligned} \mathbb{E}^{\mathbb{Q}^M} [\phi(\hat{X}_T^N)] &= \mathbb{E}^{\mathbb{Q}^M} \left[\min \left(K, \max \left(k, x \exp(rT - \frac{1}{2}v_{\hat{\pi}}^N + \sqrt{v_{\hat{\pi}}^N}F) \right) \right) \right], \\ &= \mathbb{E}^{\mathbb{Q}^M} \left[k \mathbf{1}_{\{F < a_{\hat{\pi}}^N(k)\}} + K \mathbf{1}_{\{F > a_{\hat{\pi}}^N(K)\}} + x \exp(rT - \frac{1}{2}v_{\hat{\pi}}^N + \sqrt{v_{\hat{\pi}}^N}F) \mathbf{1}_{\{a_{\hat{\pi}}^N(k) < F < a_{\hat{\pi}}^N(K)\}} \right]. \end{aligned}$$

Next, conditioning respect to $v_{\hat{\pi}}^N$ and using the independence between F and $v_{\hat{\pi}}^N$

$$\begin{aligned} E^{\mathbb{Q}^M} [\phi(\hat{X}_T^N)] &= \mathbb{E}^{\mathbb{Q}^M} \left[\mathbb{E}^{\mathbb{Q}^M} \left[k \mathbf{1}_{\{F < a_{\hat{\pi}}^N(k)\}} + K \mathbf{1}_{\{F > a_{\hat{\pi}}^N(K)\}} \right. \right. \\ &\quad \left. \left. + x \exp(rT - \frac{1}{2}v_{\hat{\pi}}^N + \sqrt{v_{\hat{\pi}}^N}F) \mathbf{1}_{\{a_{\hat{\pi}}^N(k) < F < a_{\hat{\pi}}^N(K)\}} \mid v_{\hat{\pi}}^N \right] \right], \\ &= \mathbb{E}^{\mathbb{Q}^M} \left[k \Phi_{\mathcal{N}}(a_{\hat{\pi}}^N(k)) + K \Phi_{\mathcal{N}}(-a_{\hat{\pi}}^N(K)) + x e^{rT} (\Phi_{\mathcal{N}}(b_{\hat{\pi}}^N(K)) - \Phi_{\mathcal{N}}(b_{\hat{\pi}}^N(k))) \right], \end{aligned}$$

where the functions $a_{\hat{\pi}}^N(y)$ and $b_{\hat{\pi}}^N$ are given in (7.4) and $\Phi_{\mathcal{N}}$ is the cdf of a standard Gaussian random variable. Now thanks to the law of total variance

$$\text{Var}^{\mathbb{Q}^M} (\Upsilon_{PE}^{st}(N)) = \text{Var}^{\mathbb{Q}^M} (\mathbb{E}[\Upsilon_{PE}^{st}(N) \mid v_{\hat{\pi}}^N]) + \underbrace{\mathbb{E}^{\mathbb{Q}^M} [\text{Var}^{\mathbb{Q}^M} (\Upsilon_{PE}^{st}(N)) \mid v_{\hat{\pi}}^N]}_{\geq 0},$$

where we recognize $\mathbb{E}[\Upsilon_{PE}^{st}(N) \mid v_{\hat{\pi}}^N] = \Upsilon_{PE}^{vr}(N)$ completing the proof.

D.2 Proof of Proposition 7.3

To begin, using the compensator of H_t , Fubini's Theorem and the independence of τ from X^{π^*} and \mathbf{C} we observe that

$$\begin{aligned} \mathbb{E}^{\mathbb{Q}^*} [e^{-r\tau} \phi(\tau, X_{\tau}^{\pi^*}) \mathbf{1}_{\{\tau < T\}}] &= \mathbb{E}^{\mathbb{Q}^*} \left[\int_0^T e^{-rt} \phi(t, X_t^{\pi^*}) dH_t \right] \\ &= \mathbb{E}^{\mathbb{Q}^*} \left[\int_0^T e^{-rt} \phi(t, X_t^{\pi^*}) (1 - H_t) \gamma_t dt \right] \\ &= \int_0^T e^{-rt} \mathbb{E}^{\mathbb{Q}^M} [\phi(t, X_t^{\pi^*})] \mathbb{E}^{\mathbb{P}^I} [(1 - H_t) \gamma_t] dt. \end{aligned} \tag{D1}$$

To approximate (D1), we use the discretization in (7.2) which provides an approximation of X^{π^*} along all the uniform grid $\{jh \mid j = 0, \dots, N\}$. Furthermore, we use the trapezoidal rule to discretize the Lebesgue integral in (D1). Recall that

$$\Upsilon_{TI}^{st}(N) = \frac{1}{2} \sum_{j=0}^{N-1} (\phi(jh, \widehat{X}_{jh}^N)P_{jh} + \phi((j+1)h, \widehat{X}_{(j+1)h}^N)P_{(j+1)h}),$$

see equation (7.5). Then, for all t we define $P_t = e^{-rt} \mathbb{E}^{\mathbb{P}^I}[(1 - H_t)\gamma_t]$ and get

$$\begin{aligned} \int_0^T \mathbb{E}^{\mathbb{Q}^M}[\phi(t, X_t^{\pi^*})]P_t dt &\approx \frac{1}{2} \sum_{j=0}^{N-1} \mathbb{E}^{\mathbb{Q}^M}[\phi(jh, \widehat{X}_{jh}^N)]P_{jh} + \mathbb{E}^{\mathbb{Q}^M}[\phi((j+1)h, \widehat{X}_{(j+1)h}^N)]P_{(j+1)h} \\ &= \mathbb{E}^{\mathbb{Q}^M}[\Upsilon_{TI}^{st}(N)]. \end{aligned}$$

Finally, the reminder of the proof follows the same steps as in the proof of Proposition 6.8.

References

- A. Alfonsi. High order discretization schemes for the CIR process: application to affine term structure and Heston models. *Mathematics of computation*, 79(269):209–237, 2010.
- A. Alfonsi and E. Lombardo. High order approximations of the Cox–Ingersoll–Ross process semigroup using random grids. *IMA Journal of Numerical Analysis*, 44(4):2277–2322, 2024.
- A. Alfonsi and E. Lombardo. High order approximations and simulation schemes for the log-heston process. *SIAM Journal on Financial Mathematics*, 16(2):516–544, 2025.
- M. Andersson, P. Bolton, and F. Samama. Hedging climate risk. *Financial Analysts Journal*, 72(3):13–32, 2016.
- T. Anquetin, G. Coqueret, B. Tavin, and L. Welgryn. Scopes of carbon emissions and their impact on green portfolios. *Economic modelling*, 115:105951, 2022.
- M. Bhatia, R. Gugnani, M.Z. Yaqub, P.M. Tripathi, and L. Broccardo. Emission reduction strategies and negative emission solutions-pathways, drivers, and challenges. *Journal of Cleaner Production*, 500:145263, 2025.
- P. Bolton and M. Kacperczyk. Do investors care about carbon risk? *Journal of financial economics*, 142(2):517–549, 2021.
- P. Bolton, M. Kacperczyk, and F. Samama. Net-zero carbon portfolio alignment. *Financial Analysts Journal*, 78(2):19–33, 2022.
- M. Broadie and Ö. Kaya. Exact simulation of stochastic volatility and other affine jump diffusion processes. *Operations research*, 54(2):217–231, 2006.
- N. Cai, Y. Song, and N. Chen. Exact simulation of the sabr model. *Operations Research*, 65(4):931–951, 2017.
- C. Ceci, K. Colaneri, and A. Cretarola. Hedging of unit-linked life insurance contracts with unobservable mortality hazard rate via local risk-minimization. *Insurance: Mathematics and Economics*, 60:47–60, 2015.

- C. Ceci, K. Colaneri, and A. Cretarola. Unit-linked life insurance policies: Optimal hedging in partially observable market models. *Insurance: Mathematics and Economics*, 76:149–163, 2017.
- C. Ceci, K. Colaneri, and A. Cretarola. Optimal reinsurance and investment under common shock dependence between financial and actuarial markets. *Insurance: Mathematics and Economics*, 105: 252–278, 2022.
- K. Colaneri and R. Frey. Classical solutions of the backward PIDE for markov modulated marked point processes and applications to CAT bonds. *Insurance: Mathematics and Economics*, 101: 498–507, 2021.
- J. De Spiegeleer, S. Höcht, D. Jakubowski, S. Reyners, and W. Schoutens. ESG: A new dimension in portfolio allocation. *Journal of Sustainable Finance and Investment*, 13(2):827–867, 2023.
- EIOPA. Costs and past performance report, 2023. URL https://www.eiopa.europa.eu/publications/costs-and-past-performance-report-2023_en.
- H. Föllmer and M. Schweizer. Minimal martingale measure. *Encyclopedia of Quantitative Finance*, 3: 1200–1204, 2010.
- A. Friedman. *Partial differential equations of parabolic type*. Courier Dover Publications, 2008.
- M. Görgen, A. Jacob, M. Nerlinger, R. Riordan, M. Rohleder, and M. Wilkens. Carbon risk. *Working paper*, 2020.
- S.M. Hartzmark and A.B. Sussman. Do investors value sustainability? A natural experiment examining ranking and fund flows. *The Journal of Finance*, 74(6):2789–2837, 2019.
- M. Hellmich and R. Kiesel. *Carbon Finance: A Risk Management View*. World Scientific, 2021.
- IVASS. Analysis of IBIP Policies with ESG Characteristics, 2024. URL <https://www.ivass.it/pubblicazioni-e-statistiche/pubblicazioni/altre-pubblicazioni/2024/anal>
- J. Jacod and A. N. Shiryaev. *Limit theorems for stochastic processes*, volume 2003. Berlin: Springer, 1987.
- N.V. Krylov. *Lectures on elliptic and parabolic equations in Holder spaces*, volume 12. American Mathematical Soc., 1996.
- C.J. Lagerkvist, A.K. Edenbrandt, I. Tibbelin, and Y. Wahlstedt. Preferences for sustainable and responsible equity funds - A choice experiment with Swedish private investors. *Journal of Behavioral and Experimental Finance*, 28:100406, 2020.
- T. Le Guenedal and T. Roncalli. Portfolio construction with climate risk measures. In *Climate Investing: New Strategies and Implementation Challenges*, pages 49–86. Emmanuel Jurczenko, Wiley, 2023.
- T. Møller. Risk-minimizing hedging strategies for insurance payment processes. *Finance and Stochastics*, 5:419–446, 2001.
- F. Peng, M. Yan, and S. Zhang. Optimal investment of defined contribution pension plan with environmental, social, and governance (ESG) factors in regime-switching jump diffusion models. *Communications in Statistics-Theory and Methods*, pages 1–27, 2024.

- L.C.G. Rogers. *Optimal investment*. Berlin, Heidelberg: Springer-Verlag, 2013.
- M. Schweizer. A guided tour through quadratic hedging approaches. In Musiela M. Jouini E., Cvitanic J., editor, *Option Pricing, Interest Rates and Risk Management*, page 538–574. Cambridge University Press, Cambridge, 2001.
- G. Teschl. *Ordinary Differential Equations and Dynamical Systems*. Providence, Rhode Island: American Mathematical Society, 2012.
- N. Vandaele and M. Vanmaele. A locally risk-minimizing hedging strategy for unit-linked life insurance contracts in a lévy process financial market. *Insurance: Mathematics and Economics*, 42(3):1128–1137, 2008.
- F. Verbist, J. Meus, J.A. Moncada, P. Valkering, and E. Delarue. Carbon removals meet Emission Trading System design: A precautionary path towards integration. *Energy Economics*, 145:108389, 2025.